National Library of Canada
Acquisitions and Bibliographic Services Branch
395 Wellington Street
Ottawa, Ontario
K1A 0N4

Bibliothèque nationale du Canada
Direction des acquisitions et des services bibliographiques
395, rue Wellington
Ottawa (Ontario)
K1A 0N4

Your file Votre référence

Our file Notre référence

NOTICE

The quality of this microform is heavily dependent upon the quality of the original thesis submitted for microfilming. Every effort has been made to ensure the highest quality of reproduction possible.

If pages are missing, contact the university which granted the degree.

Some pages may have indistinct print especially if the original pages were typed with a poor typewriter ribbon or if the university sent us an inferior photocopy.

Reproduction in full or in part of this microform is governed by the Canadian Copyright Act, R.S.C. 1970, c. C-30, and subsequent amendments.

AVIS

La qualité de cette microforme dépend grandement de la qualité de la thèse soumise au microfilmage. Nous avons tout fait pour assurer une qualité supérieure de reproduction.

S'il manque des pages, veuillez communiquer avec l'université qui a conféré le grade.

La qualité d'impression de certaines pages peut laisser à désirer, surtout si les pages originales ont été dactylographiées à l'aide d'un ruban usé ou si l'université nous a fait parvenir une photocopie de qualité inférieure.

La reproduction, même partielle, de cette microforme est soumise à la Loi canadienne sur le droit d'auteur, SRC 1970, c. C-30, et ses amendements subséquents.

Canada

UNIVERSITY OF ALBERTA

A STUDY OF COKE DEPOSITION IN HYDROTREATING CATALYSTS

by

SUHAS GHORPADKAR ©

A THESIS

SUBMITTED TO THE FACULTY OF GRADUATE STUDIES AND RESEARCH

IN PARTIAL FULFILLMENT OF THE REQUIREMENTS FOR THE DEGREE

OF MASTER OF SCIENCE

DEPARTMENT OF CHEMICAL ENGINEERING

EDMONTON, ALBERTA

FALL, 1993

National Library of Canada
Acquisitions and Bibliographic Services Branch
395 Wellington Street
Ottawa, Ontario
K1A 0N4

Bibliothèque nationale du Canada
Direction des acquisitions et des services bibliographiques
395, rue Wellington
Ottawa (Ontario)
K1A 0N4

Your file Votre référence

Our file Notre référence

The author has granted an irrevocable non-exclusive licence allowing the National Library of Canada to reproduce, loan, distribute or sell copies of his/her thesis by any means and in any form or format, making this thesis available to interested persons.

L'auteur a accordé une licence irrévocable et non exclusive permettant à la Bibliothèque nationale du Canada de reproduire, prêter, distribuer ou vendre des copies de sa thèse de quelque manière et sous quelque forme que ce soit pour mettre des exemplaires de cette thèse à la disposition des personnes intéressées.

The author retains ownership of the copyright in his/her thesis. Neither the thesis nor substantial extracts from it may be printed or otherwise reproduced without his/her permission.

L'auteur conserve la propriété du droit d'auteur qui protège sa thèse. Ni la thèse ni des extraits substantiels de celle-ci ne doivent être imprimés ou autrement reproduits sans son autorisation.

ISBN 0-315-88190-9

Canada

University of Alberta

Release Form

NAME OF AUTHOR : **SUHAS GHORPADKAR**

TITLE OF THESIS : **A STUDY OF COKE DEPOSITION IN HYDROTREATING CATALYSTS**

DEGREE FOR WHICH THESIS WAS PRESENTED : **MASTER OF SCIENCE**

YEAR THIS DEGREE GRANTED : **FALL, 1993**

Permission is hereby granted to THE UNIVERSITY OF ALBERTA LIBRARY to reproduce single copies of this thesis and to lend or sell such copies for private, scholarly, or scientific research purposes only.

The author reserves other publication rights, and neither the thesis nor extensive extracts from it may be printed or otherwise reproduced without the author's written permission.

Signed : Ghorpadkar

Permanent Address :
74, A, South Kasba,
Solapur 413 007
India.

Date : August 12, 1993

UNIVERSITY OF ALBERTA

FACULTY OF GRADUATE STUDIES AND RESEARCH

The undersigned certify that they have read, and recommend to the Faculty of Graduate Studies and Research for acceptance, a thesis entitled A STUDY OF COKE DEPOSITION IN HYDROTREATING CATALYSTS submitted by SUHAS GHORPADKAR in partial fulfillment of the requirements for the degree of MASTER OF SCIENCE.

M. R. Gray, Supervisor

S. E. Wanke

M. L. Wayman

Vicente A.M. Castillo

Date : July 8, 1993

ABSTRACT

A series of fifteen commercial spent catalysts and three laboratory spent catalysts used in processing of Athabasca bitumen and other feeds was examined by various microscopic techniques, including reflectance microscopy, scanning electron microscopy, energy dispersive X-ray analysis, and scanning confocal laser microscopy. The catalysts were embedded in an epoxy resin mold and were finely polished to expose a cross-section of the porous network prior to their examination.

These microscopic examinations revealed the presence of distinct domains of high reflectance values indicating coke of higher aromaticity . The existence of these domains suggested that coke deposition was not uniform but was localized. Since the γ-alumina support matrix was the only factor common to all the catalysts which showed these domains, the heterogeneity in the coke distribution was likely due to a property of the γ-alumina matrix.

In addition to bright domains, one catalyst sample showed anisotropic characteristics, which are usually associated with mesophase or liquid crystal. Since only one sample showed anisotropy, it was concluded that liquid crystal formation was not a general characteristic of the coke domains and hence mesophase formation was not the only mechanism for the formation of these domains.

The size measurements of these bright domains indicated that the mean values for different catalysts ranged from 4.68×10^{-10} to 6.44×10^{-10} m^2 in size. There was not a statistically significant difference in size of these domains among various samples and the average area of these bright domains was approximately 5.5×10^{-10} m^2, which corresponds to an average diameter of 26 μm. In two samples a distance distribution of the bright domains was observed indicative of a diffusion/reaction mechanism.

Based on the published literature and observations, a mechanism for the development of coke in distillate and residue hydrotreating catalysts was proposed.

According to this mechanism, polycyclic aromatic hydrocarbons (PAHs) were built up from simpler monoaromatics in the naphtha feed. Such PAHs would be present in heavy distillate and residue feeds. Condensation-polymerization reactions of the PAHs leading to coke were thought to have been catalyzed by high acidity sites in the γ-alumina matrix. The observed results were then explained on the basis of this mechanism.

ACKNOWLEDGEMENTS

I wish to express my sincere thanks to all the people who have helped me reaching my goal, in particular; Dr. Murray Gray, for all his guidance, help and understanding; Vicente Munoz, for his help and encouragement over the course of this study. I would also like to thank Dr. Farhad Khorasheh and Dr. Dwijen Banerjee for their valuable suggestions from time to time. The help from Alan Ayasse has been invaluable. I gratefully acknowledge the funding provided by AOSTRA for this project. Many thanks are due to Tina Barker and Henryk Kripszyk for their assistance in experiments. Finally, I appreciate the support and help given by Ramesh, Avinash and Ravi.

TABLE OF CONTENTS

Chapter			Page
List of Tables			
List of Figures			
1. Introduction			1
2. Literature Survey			2
2.1	General Discussion of Catalyst Deactivation During Hydrotreating		2
	2.1.1	Aging	2
	2.1.2	Deactivation by Poisoning	3
	2.1.3	Formation of Coke Deposits	4
	2.1.4	Formation of Metals Deposits	4
2.2	Chemistry of Coke Deposition		5
	2.2.1	Formation of Bulk Coke and Mesophase	5
	2.2.2	Physical Transformations in Formation of Mesophase	7
	2.2.3	Mesophase Development in Coking of Aromatic Oils	8
	2.2.4	Factors Controlling the Size and Anisotropic Characteristics of Coke	8
2.3	Deposition of Coke and the Role of Acidity of the Support		9
	2.3.1	Mechanisms of Acidity Enhancement in	

Hydrated Alumina 10
2.3.2 Effect of Enhanced Lewis Acidity on Coke Formation 12
2.3.3 Acidic Support and Mesophase Development 12
2.4 Chemistry of Metals Deposition 13
2.5 Kinetics of Coke Formation 14
2.6 Techniques Used to Examine Coke Deposits 15
2.6.1 Reflectance Measurements 15
2.6.2 Fluorescence Measurements 16
2.6.3 Optical Characteristics of Coke 16
2.6.3.1 Methods for Observation of Mesophase 17
3. Experimental Materials and Methods 18
3.1 Catalyst Materials and Data Sheet 18
3.1.1 Spent Catalysts from Industrial Reactors 18
3.1.2 Spent Catalysts from Laboratory Reactors 22
3.2 Preparation of Catalyst Samples 25
3.2.1 Polishing of Catalyst Samples 25
3.3 Microscopic Analysis of the Catalysts 25
3.3.1 Optical Microscopy 26
3.3.2 Introduction to Confocal Laser Scanning Microscopy (CLSM) 27
3.3.3 Scanning Electron Microscopy and Energy Dispersive X-ray Analysis 28

3.3.4 Characterization by SEM and EDX Analysis 28

4. Results 30

4.1 Introduction to Optical Microscopy Examination of Carbonaceous Materials 30

4.2 Qualitative Results of Optical Microscopy 30

4.2.1 Reflectance of Naphtha Catalyst Pellets 30

4.2.2 Reflectance of Middle Distillate Catalyst Pellets 32

4.2.3 Optical Microscopy of Bitumen Catalyst Pellets 32

4.2.4 Fluorescence Microscopy of Catalyst Pellets 38

4.2.5 Qualitative Results of CLSM Examination 38

4.3 Quantitative Results of Optical Microscopy 43

4.3.1 Reflectance Measurements 43

4.3.2 Area Measurements of Bright Spots 49

4.3.3 Area Distribution Measurements 49

4.3.4 Distance Distribution Measurements 56

4.4 Scanning Electron Microscopy and Energy Dispersive X-ray Analysis of Catalyst Pellets 58

4.4.1 SEM Elemental Analysis by EDX for Naphtha A 58

4.4.2 SEM Elemental Analysis by EDX for Bitumen A 58

4.4.3 SEM Elemental Analysis by EDX for Silica A 62

5. Discussion 64

5.1 Heterogeneity in Carbonaceous Deposits 64

5.1.1 Anisotropy of Bright Domains 65

5.1.2 Fluorescence Characteristics of Bright Domains 65

5.1.3 Size of Bright Domains 66

5.1.4 Area Ratio of Bright Domains 66

5.1.5 Distance Distribution of Bright Domains 67

5.1.6 EDX Analysis Results in case of Naphtha A 67

5.2 Possible Causes of Heterogeneous Distribution of Coke 67

5.2.1 Mesophase Analogy 67

5.2.2 Heterogeneity of Alumina Domains 68

5.2.3 Comparison Between the Two Hypotheses 68

5.3 Development of Coke in Distillates Hydrotreating Catalysts 70

5.3.1 Implications of Alumina Domains Mechanism in case of Naphtha Catalysts 75

5.3.2 Implications of Alumina Domains Mechanism in case of Gas-oil and Middle Distillates Catalysts 76

5.4 Development of Coke in Residue Hydrotreating Catalysts 78

5.5 Implications of Heterogeneous Coking 80

6. Conclusions 81

7. Recommendations for Future Work 82

7.1 Role of P and Ca in Modifying the Surface Properties 82

7.2 Regeneration of Spent Catalysts 83

8. List of References 84

Appendix I 92

LIST OF TABLES

Table		Page
3.1	Physical Property Data of the Catalysts	23
3.2	Elemental Analysis Data of the Catalysts	24
4.1	Catalysts Showing Bright Regions	44
4.2	Mean Random Reflectance Values for Naphtha A and Naphtha B Catalysts	45
4.3	Statistical Data of the Reflectance Measurements of the Laboratory Spent Catalysts	48
4.4	Statistical Data of the Reflectance Measurements of the Commercially Spent Catalysts	48
4.5	Area Ratios and Average Areas of Bright Spots	50
4.6	Results of SEM Analysis for Naphtha A	59
4.7	Results of SEM Analysis for Bitumen A	59
4.8	Results of SEM Analysis for Naphtha A	59

LIST OF FIGURES

Figure		Page
2.1	Mechanism of Acidity Enhancement in Alumina	11
4.1	Naphtha A under Bright Field Illumination at 300 X magnification	31
4.2	Part of Figure 4.1 at 1900 X magnification	31
4.3	Naphtha B under Bright Field Illumination at 300 X magnification	33
4.4	Naphtha A under Cross-polarized light at 300 X magnification	33
4.5	MD-A under polarized light, oil immersion at 600 X magnification	34
4.6	Bitumen A at 220 X magnification	35
4.7	CSTR-1 under partially cross-polarized light at 220 X magnification	35
4.8	CSTR-2 under polarized light, oil immersion at 220 X magnification	36
4.9	Figure 4.8 at 1650 X magnification	36
4.10	Figure 4.8 at 1650 X magnification	37
4.11	CSTR-3 under polarized light, oil immersion at 1650 X magnification	37
4.12	Naphtha A at 420 X magnification	39
4.13	Figure 4.12 under a blue light source	39
4.14	CSTR-2 under cross-polarized light at 1900 X magnification	40
4.15	Figure 4.14 under blue light (450-490 nm)	40
4.16	CLSM photograph of CSTR-1 with 64 optical sections at 300 X magnification	41
4.17	CLSM photograph of CSTR-3 with 38 optical sections at 220 X magnification	42

4.18	Reflectance Histograms for Naphtha A	46
4.19	Reflectance Histograms for Naphtha B	47
4.20	Number Fraction of Bright Spots vs. Area Range Histogram for Naphtha A	51
4.21	Number Fraction of Bright Spots vs. Area Range Histogram for Naphtha B	52
4.22	Number Fraction of Bright Spots vs. Area Range Histogram for MD-A	53
4.23	Number Fraction of Bright Spots vs. Area Range Histogram for Gas-oil A	54
4.24	Number Fraction of Bright Spots vs. Area Range Histogram for Gas-oil C	55
4.25	Number Fraction of Bright Spots vs. Dimensionless Distance Histograms for MD-A and Gas-oil C	57
4.26	EDX Traverses for Naphtha A	60
4.27	EDX Traverses for Bitumen A	61
4.28	EDX Traverses for Silica A	63
5.1	Condensation-polymerization Reactions between Monoaromatics and Olefins	71,72,73
5.2	Ring Closure Reactions Sequence	74
5.3	Asphaltenes in Micellar Form	79

CHAPTER 1 : INTRODUCTION

Catalyst deactivation due to coke formation is an important technological and economical problem in petroleum refining and in the petrochemical industry. Remedies to catalyst deactivation are sought by a variety of strategies involving modification of catalyst surface composition and/or by manipulation of the reaction environment which often limits the yield due to thermodynamic constraints.

Obviously the first remedy to deactivation, that is, activity alteration to produce coking-resistant catalyst, is an ongoing research effort in process development. However, the current catalysts are optimized for desulfurization of feeds, and not nitrogen removal and saturation of aromatics. An ideal catalyst should have good activity for nitrogen removal and hydrogenation of aromatics, and promote cracking of the feed and limit hydrogenation by giving equilibrium between reactants and products.

Most catalyst development has been focused on the cracking activity by adding acidic functions like fluoride or chloride to the γ-alumina support. The higher acidity correlates with cracking and conversion of phenols or nitrogen bases. These catalysts have not been optimized for upgrading Alberta bitumen which has higher nitrogen content. Acidic sites on the catalyst surface promote coke formation and dramatic accumulation of nitrogen and oxygen.

The purpose of this study was to examine the microscopic nature of coke deposition in commercial as well as laboratory spent hydrotreating catalysts and based on the results of examination try to understand the chemistry of coke formation.

CHAPTER 2 : LITERATURE SURVEY

There is extensive literature concerned with deactivation of catalysts and hence the focus of this literature survey will be deactivation of hydrotreating catalysts. This chapter will deal with the following aspects of deactivation of hydrotreating catalysts:

1. General discussion of catalyst deactivation during hydrotreating
2. Chemistry of coke and metal deposition
3. Discussion of various microscopic techniques used in characterizing coke and metal deposition

2.1 General Discussion of Catalyst Deactivation during Hydrotreating

The success of many commercial operations is markedly affected by use of an active and stable catalyst. In refinery practice, cracking, reforming, hydrodesulfurization, hydrodenitrogenation and hydrotreating are the most common processes requiring a catalyst. To achieve high performance, it is essential that the catalyst either resist deactivation for as long as possible, or that the nature of deactivation be such that the catalyst can be easily regenerated and returned to operation. In hydrotreating operations the catalyst is continuously deactivated. The factors responsible for loss of catalyst activity can be grouped into the following categories (Furimsky, 1979) :

1. Aging
2. Poisoning
3. Formation of coke deposits
4. Formation of metals deposits

2.1.1 Aging

Aging, or sintering, of supported metal catalysts, refers to the loss of catalytic metal sites due to the agglomeration of metal, resulting in the growth of metal particles (Wanke *et al.*, 1987). These changes in the catalyst structure are usually the result of

prolonged exposure to high temperatures. The active ingredients, which are spread out on the surface of the support in layers, tend to diffuse into or mix with the support after a long exposure to the high temperatures. For promoted molybdate catalysts, usually used in hydrotreating distillates, Ni is reported to have higher rates of diffusion than Co (Gates, 1978). Wanke *et al.* (1987) have presented a detailed discussion on sintering of supported metal catalysts.

2.1.2 Deactivation by Poisoning

Poisoning refers to the irreversible or competitive reversible adsorption of inhibitory compounds on the surface of the catalyst (Butt, 1987). Because they have strong interaction with the surface, poisons delay the renewal of active sites. Preferentially adsorbed species are either present in the feedstocks or formed during catalytic hydrotreating reactions. For example, a decrease of activity for thiophene was observed as the result of strong adsorption of benzo-thiophene on the surface of molybdenum catalyst (Furimsky and Amberg, 1976). In the same study, it was also possible to desorb benzo-thiophene and weaken its interaction with the surface by increasing the temperature. This type of poisoning is called as reversible poisoning.

Active sites are characterized by their acidity or basicity. Certain species poison acidic or basic sites selectively, while leaving the other intact. Acidic sites, which are present on zeolite and to a lesser extent also on supported molybdate catalysts, are easily poisoned by basic nitrogen compounds (Furimsky, 1979).

A number of catalysts are extremely sensitive to nitrogen, sulfur and oxygen compounds, particularly H_2S, NH_3 and H_2O, which are formed in hydrotreatment from the S, N and O always present in petroleum feedstocks. NH_3 and H_2O are known to be strongly adsorbed on the surface of molybdate catalysts (Lipsch and Schuit, 1969). For hydrotreating distillate fractions, sulfided Co/Mo or Ni/Mo catalysts are generally used and these catalysts are relatively insensitive to poisoning by sulfur (Sie, 1980). Apart from poisoning by trace metals (V, Ni), which is much more a problem in residue processing,

deactivation by silicon is one of the relatively rare instances of hydrotreating catalyst poisoning (Sie, 1980). There is a large amount of literature available on this subject and a recent review (Schlosser, 1988) deals thoroughly with the deactivation by poisons, which are present either in the feedstocks or formed in hydrotreating reactions.

2.1.3 Formation of Coke Deposits

Various carbonaceous species are produced during the processing of carbon-containing feedstocks over supported-metal catalysts. The reactions of these species can lead to products or alternatively to coke and other forms of carbon which deactivate the catalyst. Coke is a hydrogen deficient residue which forms on catalyst surfaces and is insoluble in many common solvents like toluene, methylene chloride and THF. These deposits are formed by a variety of side reactions associated with cracking, and their formation is inhibited by hydrogen. The side reactions which give rise to the formation of coke are usually disproportionation-polymerization reactions and are called coking reactions. Coke typically consists of a polyaromatic condensed-ring structure, and it is formed in almost all catalytic hydrocarbon conversion processes. Deactivation by coke can be due to blockage of metal sites, encapsulation of metal crystallites, and blockage of pores in the catalyst support (Bell, 1987). The extent and rate of coke formation varies with the type of operation. It is generally expected that coke levels are higher for catalytic cracking than for hydrotreating, since during hydrotreating, hydrogenation and sulfur, nitrogen and oxygen removals are the main reactions and these are not coking reactions. This trend was confirmed by decreases in coke levels with improving catalyst activity for the removal of S, N and O from a non-asphaltene feedstock (Ternan *et al.*, 1979). However, the coke deposits have been found to contain higher concentrations of heteroatoms and the role played by heteroatoms in the coking reactions is still unclear. For a complete discussion of the mechanisms and chemistry of coke deposits, refer to Section 2.2.

2.1.4 Formation of Metals Deposits

High-molecular weight compounds of V and Ni, and of other metals to a lesser extent, are found in the residue fraction of most feedstocks. During hydrotreating these molecules decompose, resulting in the deposition of metals on the catalyst surface. These metals in the feed deposit within the pores of the catalyst pellet as metal sulfides. These deposits, though usually not as active as the catalytic sites originally present in the catalyst, are active demetallization catalysts. The accumulation of metal containing deposits over a long period of operation causes irreversible catalyst deactivation (Pereira, 1990). V and Ni usually concentrate in the coke layers and the deactivation effect of metals on the catalyst surface is usually irreversible. For a more complete discussion on the mechanisms of metals deposition, refer to Section 2.2.

2.2 Chemistry of Coke Deposition

2.2.1 Formation of Bulk Coke and Mesophase

Coke deposition begins with the adsorption of coke precursors on catalyst surface. Highly unsaturated hydrocarbons having high molecular weights are strongly adsorbed on catalytic surfaces. Their presence on a surface in high concentration, their ease of protonation, and the stability of the resultant carbonium ion best explain the observation that aromatics have high coke forming tendencies. For paraffins, both the rate of cracking and the rate of coke formation increase as the molecular weight of the reactant increases, and for paraffins of a particular carbon number, the coke formation rate correlates well with paraffin reactivity (Nace, 1969). This result suggests that the rate of coke formation may be tied to the rate of olefin formation and to the overall hydrogen balance for the system. The extent of adsorption of these precursors depends on the strength of interaction between surface and the species.

In the case of petroleum feedstocks, polar S-, N- and O-containing compounds will certainly tend to be adsorbed more strongly than neutral hydrocarbons (Furimsky, 1979). The high accumulation of S, N and O in coke deposits (Furimsky, 1978; Wukasch

and Rase, 1982; Choi and Gray, 1988) confirms that the molecules containing heteroatoms are important precursors of coke, when present in feed. For example, methanol extracts from a naphtha catalyst contained 3.7-4% N, compared to 0.3% in the coker naphtha feed to the reactor (Choi and Gray, 1988). The high N/C ratio in the coke layer formed during hydrotreatment of gas oil containing no asphaltenes and a high concentration of heterocyclic compounds (Furimsky, 1979) suggests that N-containing compounds are important coke precursors. Analysis of solvent extracts from spent catalysts by potentiometric titration, in combination with reduction by $LiAlH_4$, and also by IR confirmed the presence of amides such as quinoline (Choi and Gray, 1988) in coke deposits. Wukasch and Rase (1982) showed that the exterior of spent gas oil catalyst was higher in carbon, while the interior was higher in nitrogen. Hence, the role of O- and N-containing compounds is significant in the deactivation process. Also, the amount of carbon deposited does not increase gradually, but reaches its maximum steady-state value of about 15-30% in a short period (Thakur and Thomas, 1985; Diez *et al.*, 1990). The carbon content increases from the entrance to the exit of the fixed bed reactor and it is uniformly distributed throughout the catalyst pellet for distillate hydrotreating, while it is concentrated at the edges of the pellet for heavy oils, such as asphaltenes, processing (Tamm *et al.*, 1981; Stanulonis *et al.*, 1976).

The carbonaceous deposits found on catalysts used to process different feedstocks vary in structural composition and approach the character of graphite depending on the feedstock involved and the process conditions and time-on-stream. Although these carbonaceous deposits have been called coke, recent work with ^{13}C-NMR suggests that a wide variety of carbon deposits can occur on catalyst surfaces used to treat distillates (Egiebor *et al.*, 1989). Several studies by Furimsky (1978; 1982) revealed the presence of polycondensed aromatics and aliphatic carbons in solvent extracts from a Co-Mo catalyst used in hydrotreating coal-derived liquids. Solid-state ^{13}C-NMR studies have shown that catalysts near the entrance of the reactor contained deposits with a high content of

aliphatic carbon, from 30-50 % of the total, as compared to 60-70 % in the feed. The high-molecular weight methanol extract from a naphtha catalyst contained even more aliphatic carbon at 78 % (Choi and Gray, 1988). Catalysts at the end of the reactor contained deposits with a high carbon content and a higher aromaticity, as much as 99 % in a naphtha hydrotreating catalyst (Egiebor *et al.*, 1989). These data indicate that two modes of deactivation may occur, one due to heteroatomic species near the inlet, giving a N- and O-rich deposit, and a second lower in the reactor due to higher temperature and lower hydrogen pressure.

The second mode of catalyst deactivation has been likened to the formation of mesophase. Brooks and Taylor (1965) first recognized the significant role of the mesophase transformation which takes place in graphitizable organic materials during carbonization at temperatures between 400 and 500^0C. The carbonaceous mesophase is the result of a liquid-state structural transformation in which the larger planar aromatic molecules produced by the pyrolysis reactions are aligned parallel to form an anisotropic liquid crystal (Dubois *et al.*, 1970). It has been reported that the principal features of the morphology of the carbons and graphites produced by liquid-state pyrolysis are established by the molecular alignment, coalescence, and flow which occur in the carbonaceous mesophase during the short interval of time and temperature in which it is liquid or plastic (Kipling *et al.*, 1966). They also reported that the effects of further heat-treatment of the hardened, or coked, mesophase constitute microstructural modifications which are minor by comparison with those resulting directly from mesophase transformation.

2.2.2 Physical Transformations in Formation of Mesophase

In the carbonization of coal-tar and petroleum pitches, Dubois *et al.* (1970) observed two regimes leading to the formation of mesophase : the liquid range, from the formation of viscous liquid crystal to its hardening to an effectively solid coke; and the solid range, during which the hard coke gradually softens to crystalline graphite. Dubois *et al.* (1970) also reported that during the short liquid range the morphological elements of

bulk mesophase are established by three mechanisms :

1. Nucleation and growth of spherules of liquid mesophase
2. Coalescence of the spherules and subsequent rearrangement to form bulk mesophase
3. Deformation of viscous mesophase by bubble percolation or other stresses leading to the folding of the layers or increases in the density of layer-stacking defects.

No nucleation, in the traditional sense, is necessary for the initiation of liquid crystal growth (Marsh, 1973). The liquid structures grow by stacking of the lamellar molecules produced due to condensation and rearrangement reactions. To minimize surface energy, minimum interfacial areas are favored and the liquid crystals are observed initially as spheres (Brooks and Taylor, 1968).

2.2.3 Mesophase Development in Coking of Aromatic Oils

Thermal coking of aromatic oils gives an orientation of aromatic molecules that can be seen through a microscope (Beuther *et al.*, 1980). Beuther *et al.* reported that when aromatic oils are heated, the naphthenes are either cracked or dehydrogenated and aromatics concentrates orient themselves in clusters. The authors likened this orientation of aromatics in stacked layers to the formation of liquid crystal or mesophase formed in the pyrolysis reaction of graphitizable materials. Beuther *et al.* also reported that coking of the decant oil (refractory oil that resists further conversion), in the absence of alumina support, resulted in liquid crystals in about 5 to 10 minutes at 400 to 410^0C. These mesophase crystals grew by coalescence until the size reached 100 μm. In the presence of γ-alumina support, the size reached was smaller by an order of magnitude compared to the one in absence of γ-alumina.

2.2.4 Factors Controlling the Size and Anisotropic Characteristics of Coke

The growth and coalescence pattern of the liquid crystals determines the final area occupied by coke. Marsh (1973) reported that in carbonization of petroleum pitch, the

mesophase spheres originate at different times, grow at different rates producing a large range of size of spheres. Coalescence does not occur uniformly and ultimately a range of size of coke domains is found. On the other hand, Kipling *et al.* (1966) reported that in carbons prepared from heterocyclic compounds, the spheres are initiated uniformly but never grow beyond a relatively small size. On coalescence, a fine mosaic of anisotropic units of size *ca.* 2 μm results. The temperature range of fluidity of mesophase and the mobility of the constituent molecules thus seems to affect the growth process. This conclusion is supported by Marsh (1973) who reported that carbonization of large aromatic molecules like dibenzanthrone and pyranthrone produced small anisotropic units, 0.2 μm to 3 μm in diameter, compared to 25 μm from carbonization of naphthalene. Thus, the rate of formation of liquid crystals is controlled by both the chemical rate of formation of suitably shaped molecules and the mobility (diminishing with increasing size) of these molecules in the plastic phase of carbonization.

The presence of S-, N-, and O-containing groups in the feed is shown to have an influence on the growth process after they exceed a threshold value of concentration (Marsh, 1973; Weinberg and Yen, 1982). Higher concentrations of heterocyclics containing these groups have been reported (Marsh, 1973; Kipling *et al.*, 1966) to retard the growth process by increasing the viscosity and decreasing the plastic or liquid range of the mesophase, resulting in decreased ability to form anisotropic carbon. Kipling *et al.* (1966) attributed these effects to the cross- linking reactions producing non-planar, high molecular weight configurations.

Apart from the above factors, other factors like presence of solid surfaces within the liquid phase, the presence of inerts, diffusional restrictions on the movement of the liquid stage, and the acidity of the support play an important role in the growth and coalescence of mesophase crystals. The role of acidity will be discussed in details because of its paramount importance in the deactivation of catalysts.

2.3 Deposition of Coke and the Role of Acidity of The Support

Gamma-type aluminas are almost exclusively used as catalyst supports in hydrotreating operations, since they produce less coke than eta- or other type of alumina configurations (Beuther *et al.*, 1980). These aluminas are hydrated to increase their surface area and they are weakly acidic (Gates *et al.*, 1979). There is more emphasis on increasing the acidity of alumina surface by treating them with HCl or HF, since increased acidity means higher hydrocracking and hydrodenitrogenation activity (Weisser and Landa, 1973). Stronger acidic sites are also required for reforming reactions such as disproportionation, dealkylation and isomerization which are believed to occur via carbonium ion mechanism (Boorman *et al.*, 1985).

2.3.1 Mechanisms of Acidity Enhancements in Hydrated Alumina

The hydrated alumina exists in parallel planes of Al^{3+} and OH^- ions forming layers (Gates *et al.*, 1979). The acidity of the OH groups on the surface can be enhanced by treating with HCl or HF. The proximity of Cl^- ions sets up an electronic asymmetry which draws electrons from the O-H bond, increasing the acidity of the group (Gates *et al.*, 1979). Figure 2.1 shows this mechanism.

Apart from chlorine, addition of fluoride ion has been reported to enhance the acidity of alumina (Boorman *et al.*, 1987) and also of Co-Mo-Al_2O_3 catalysts used in hydrocracking of Athabasca bitumen (Boorman *et al.*, 1982).

Experiments performed with adsorption of pyridine on γ-alumina indicate that both fluoride ion and MoO_3 increase the Lewis acidity (Lewis acid : which can accept an electron pair) of alumina, while CoO leaves this property unaffected (Boorman *et al.*, 1985). They also reported that the addition of fluoride ion initiates some Brønsted acidity (Brønsted acid : which can donate a proton) and enhances the strength of Lewis acidity. The presence of MoO_3 introduces another group of Brønsted acidity but this Brønsted acidity does not enhance significantly the reactivity of catalyst for cumene cracking to benzene (Boorman *et al.*, 1985). However, it has been reported that these Lewis acid sites are distributed over the surface of the catalyst and they also vary in their strengths (Gates

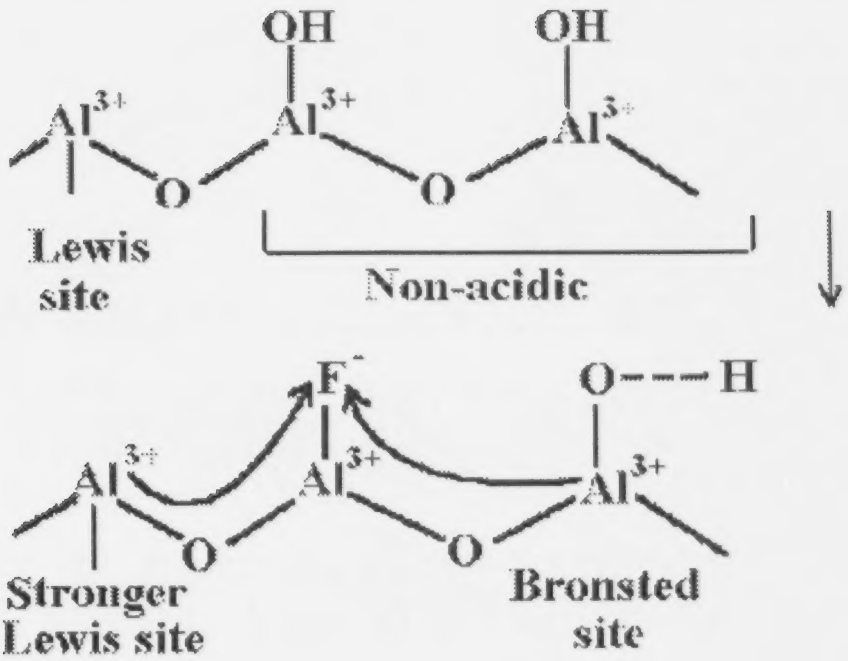

Figure 2.1 Mechanism of Acidity Enhancement in Alumina

et al., 1979; Knözinger and Ratnasaamy, 1978; Mills *et al.*, 1950; Pines and Haag, 1960). It has also been reported that Ni/Mo γ-alumina hydrotreating catalysts had distribution of three types of acid centres viz., strong, intermediate and weakly acidic centres (Yoon *et al.*, 1991). These authors also reported that in coal liquefaction with these catalysts, weakly acidic sites improved the liquefaction yields.

2.3.2. Effect of Enhanced Lewis Acidity on Coke Formation

It has been reported that during dehydration of n-butanol and 2-ethylhexanol over SiO_2-Al_2O_3, the strongly acidic centres diminished in a greater proportion than the weak centres (Aguayo *et al.*, 1987). The fact that the strong centres are more affected by the deposition of coke has led many researchers (Aguayo *et al.*, 1987; Butt, 1972; Masuyama *et al.*, 1990) to equate the deposition of coke with strong acidity. Furimsky (1987) reported that these strong acidic sites promote coke formation and Choi and Gray (1988) reported that they also promote dramatic accumulation of nitrogen and oxygen even in a hydrogen rich system. However, there is a scarcity of published literature on this subject and further work in this area is needed.

2.3.3. Acidic Support and Mesophase Development

Beuther *et al.*(1980) reported that in the presence of γ-alumina, there was a large decrease in the size of the mesophase crystals formed in the coking of Edmonton decant oil (refractory oil which resists further treatment) compared to the size in absence of alumina. The coking experiments were carried out adiabatically and for 120 days maximum. The decrease in the size of mesophase crystals was reported to be due to the formation of coke on the alumina surface. This coke was thought to inhibit the growth of mesophase because of the depletion of precursors by conversion to coke before the coalescence stage required for the formation of larger mesophase crystals. Also, the cracking activity of these aluminas was thought be depleting the reservoir of decant oil by forming lighter hydrocarbons. However, these authors did not comment on the acidity of the aluminas and also the effect of longer service time on γ-alumina.

The following can be concluded about the carbonaceous deposits on hydrocracking and hydrotreating catalysts from the published literature :

1. The amount of carbonaceous deposits on catalysts is greater at the exit of the reactor than at the entrance, due to higher temperature and lower hydrogen partial pressure at the exit.

2. The carbonaceous deposits at the entrance of the reactor contain more heteroatoms (S, N and O) than at the exit because the feed is enriched in heteroatom content when it enters the reactor.

3. The carbonaceous deposits contain more aliphatic carbon at the entrance of the reactor and more aromatic carbon at the exit of the reactor. This trend is due to the higher pressure of hydrogen at the inlet which partially hydrogenates the unsaturated heteroatom containing groups, once heteroatoms are adsorbed to the catalyst surface.

4. The rate of coke formation increases with increasing acid strength of the catalyst and with increasing base strength of the hydrocarbon reactant, i.e., with increasing the ease of formation and the stability of the carbonium ion.

2.4 Chemistry of Metals Deposition

Metal deposits should be discussed separately from the coke deposits because their deactivation effect on the catalyst surface is usually irreversible (Furimsky, 1979). In heavy petroleum feedstocks, Ni, V, and Fe are the major metal contaminants and their decomposition (decomposition of metals-containing groups on the surface of the catalysts in presence of hydrogen is called a hydrodemetallization reaction) under hydrotreating conditions leaves metal deposits in the catalyst pores (Thakur and Thomas, 1984). Heavy gas oils contain only low concentrations of metals (Ni, V and Fe) which are easily removed by a guard bed, so that accumulation of metals is not a primary mechanism for deactivation in treating distillates. The deposition of these metals is much slower than that of the carbonaceous materials. In a fixed bed reactor, metal deposition decreases from the inlet to the exit of the reactor (Nishijima *et al.*, 1987). The metal deposits are generally

found to be concentrated at the external surface of the catalyst extrudate (Nashijima *et al.*, 1987). In the hydrotreating of petroleum residue, the metals are in the form of metal sulfides, while in coal-derived liquids the metals are in the form of oxides, carbonates or sulfates (Fleisch, 1987).

The understanding of chemical structure of the organo-metallic compounds in feedstocks is essential to understanding deactivation due to metals deposition. V and Ni are shown to exist in the porphyrin as well as ionic forms (Furimsky, 1979). It has been shown that metals originating from ionic form are much more reactive in catalyzing the formation of coke and gas (Cimbalo *et al.*, 1972). Also, Ni compounds present in crudes are known to be more weakly adsorbed than V compounds. The rate of V accumulation in coke is therefore higher than that of Ni (Furimsky, 1979). This result was confirmed by a higher V/Ni ratio, which was about 9, related to the carbonaceous deposits compared to the concentrations of metals in the feed, which was about 3 (Furimsky, 1978). V compounds, because of their strong interaction with the surface, concentrate on the surface and cause serious deactivation by blocking the active sites.

It has recently been shown that the carbonaceous material contains organic sulfur as well as metal sulfide sulfur (van Doorn *et al.*, 1992).The sulfur was measured by temperature programmed reduction method using hydrogen and the amount of organic sulfur increased as the feed got heavier.

2.5 Kinetics of Coke Formation

Several kinetic models have been proposed to explain deactivation by coking. In the earliest work by Voorhies (1945), he proposed a time-on-stream correlation relating the weight of coke on the catalyst to the time of catalyst utilization.

$$C_c = a\,(t_c)^b$$

where C_c is the weight percent of coke on the catalyst, a is a dimensionless correlation parameter, tc is time-on-stream, b is another dimensionless correlation parameter.

A number of different forms for time-on-stream correlations have been proposed

since then, which give similar results in reactor analysis to the one presented above. However, this form of correlation gave rise to two incorrect inferences; that coke deposition is diffusion-limited and not dependent upon space velocity. The former inference was deduced from the fact that the exponent b of the above equation is often near 0.5, and the latter inference arose because early experiments did not cover a very large range of space velocities (Butt, 1981). Ozawa and Bischoff (1968) refuted the first claim by reporting values of b varying from 0.55 to 0.92 for ethylene cracking on a commercial silica/alumina catalyst in the temperature range 620-770 K. Butt (1972) refuted the second claim by showing dependence of coke deposition on space velocity.

2.6 Techniques Used to Examine Coke Deposits

The following section introduces the various microscopic techniques used in qualitative characterization of the coke deposits in the course of this study.

Optical microscopy has been widely used for observation of the surface of cokes from petroleum and coal. Optical microscopy can be used to observe several characteristics, as follows : reflectance, isotropic or anisotropic character of the coke, fluorescence, morphology and color.

2.6.1 Reflectance Measurements

The reflectance of a surface is related to the refraction and absorption indices by the Beer-Fresnel equation (Gray and Cathcart, 1966) :

$$R = \frac{I(r)}{I(i)} = \frac{(n-n_0)^2 + (n^2k^2)}{(n+n_0)^2 + (n^2k^2)}$$

where R = reflectance,

$I(r)$ = intensity of reflected beam

$I(i)$ = intensity of the incident beam

n = index of refraction, k = index of absorption

n_0 = index of refraction of immersion media (air, water or oil)

The refraction and absorption indices are related to the molecular structure of the specimen. Reflectance serves, therefore, as an indirect tool for assessing the aromaticity of carbonaceous solids (Stach *et al.*, 1982). With increasing processing temperature, the aromaticity of coke formed increases with the consequent rise in the reflectance values (Stach *et al.*, 1982; Weinberg and Yen, 1982).

2.6.2 Fluorescence Measurements

The increase in the aromaticity of the coke increases the reflectance values. Concurrent with the increase of reflectance, the fluorescent properties of some of the coke precursors are reduced or destroyed. A highly conjugated double bond system formed by a combination of aromatic and aliphatic fractions is responsible for fluorescence from carbonaceous deposits and adsorbed fluorphores (White and Argauer, 1970). The disproportionation, condensation and polymerization reactions occurring during coke formation cause a reduction in the fluorescent intensity and shift the wavelength of maximum intensity (λ_{maxima}) to a longer wavelength or bathochromic shift (White and Argauer, 1970).

During the pyrolysis of graphitizable materials, like coal-tar and petroleum coker feedstocks, layers of aromatic sheets become aligned leading to the formation of a liquid crystal, the carbonaceous "mesophase". Larger planar aromatic molecules dominate in mesophase structures (Dubois *et al.*, 1970). With increasing temperature, the mesophase crystals grow and coalesce and are optically anisotropic (Sanada *et al.*, 1973). At the mesophase stage, the fluorescent properties are completely eliminated and these mesophase crystals show higher reflectance values than the surrounding isotropic coke (Dubois *et al.*, 1970).

2.6.3 Optical Characteristics of Cokes

The isotropic or anisotropic character of the coke deposits depends upon the chemical composition of the feed, reaction rate, temperature and residence time (Stach *et al.*, 1982). In general, relatively planar aromatic molecules produce anisotropic coke

whereas non-planar configurations, of high molecular weight, produce isotropic coke (Marsh, 1973). Isotropy is due to steric hindrance which prevents the alignment of the molecules to form the nematic (thread-like structure, the opposite of smectic or soap-like structure) mesophase giving rise to the anisotropic coke (Weinberg and Yen, 1982). Polar groups containing O and S favor the formation of isotropic coke by producing non-planar free radicals which cross-link the products (Weinberg and Yen, 1982).

2.6.3.1 Methods for Observation of Mesophase

Polarized light microscopy is invariably used in the studies of mechanisms of carbonization and graphitization. The value of polarized light microscopy stems from the fact that the strong optical anisotropy characteristic of graphite crystal begins with the parallel alignment of aromatic molecules to form carbonaceous mesophase (Dubois *et al.*, 1970). Accordingly, the polarized light response on a polished section can be used to identify the orientations of mesophase layers relative to the plane of section (Gray and Cathcart, 1966). Also, the sensitive-tint technique (a modification of polarized light microscopy) has been reported to be particularly useful in illustrating the orientational relationships which exist between the mesophase layers and various substrate materials (Brooks and Taylor, 1965).

The reflectance is a property of molecular structure of specimen. Hence reflectance measurements can be used as an indirect method of assessing the aromaticity of the carbonaceous deposits. The aromaticity, in turn, depends upon the chemistry of feed components and temperature and residence time history. Thus combining the mesophase phenomenon with reflectance measurements can be used to explain the mesophase development and subsequent deactivation by coking in hydrocracking and hydrotreating catalysts.

CHAPTER 3 : EXPERIMENTAL MATERIALS AND METHODS

To study deactivation in hydrotreating catalysts, fifteen commercial spent catalysts were analyzed in the course of this study. It would be appropriate at this point to outline the details about these catalysts. In some cases the data were not available and it has been noted in the following data sheet.

3.1 Catalyst Materials and Data Sheet

The following list gives the relevant data for each catalyst and the catalysts are grouped according to their feedstock. The physical properties of the fresh catalysts and elemental analysis of the spent catalysts are listed in Tables 3.1 and 3.2 respectively.

3.1.1 Spent Catalysts from Industrial Reactors

1. Naphtha A

Provided by	: Syncrude Canada Ltd.
Supplier Code	: ARS Composite C-3 MH-705
Primary purpose	: Hydrotreating naphtha
Feedstock	: Naphtha
Catalyst Composition	: Ni/Mo on γ-alumina
Time-on-stream	: 12-14 months in the first naphtha hydrotreating reactor
Temperature	: 280-330 ^{0}C
Pressure	: 5.5-6.9 MPa

2. Naphtha B

Provided by	: Syncrude Canada Ltd.
Supplier Code	: ARS Composite C-4 MH-707
Primary purpose	: Hydrotreating naphtha
Feedstock	: Naphtha
Catalyst Composition	: Ni/Mo on γ-alumina
Time-on-stream	: 12-14 months in the second naphtha hydrotreating reactor
Temperature	: 400-450 ^{0}C
Pressure	: 5.5-6.9 MPa

3. Naphtha D

Provided by	: Syncrude Canada Ltd.
Supplier Code	: TK 711
Primary purpose	: Pretreatment of residual oils for reduction of metals, asphaltenes.
Feedstock	: naphtha
Catalyst Composition	: Ni/Mo on γ-alumina
Time-on-stream	: 18 months
Temperature	: **not available**
Pressure	: **not available**

4. Naphtha E

Provided by	: Syncrude Canada Ltd.
Supplier Code	: 13-1 Naphtha Canister NH Comp # 4 HDS-3A (C)
Primary purpose	: Hydrodesulfurization of naphtha
Feedstock	: Naphtha
Catalyst Composition	: Co/Mo on γ-alumina
Time-on-stream	: 2 years
Temperature	: **not available**
Pressure	: **not available**

5. Naphtha F

Provided by	: Esso Petroleum Canada
Supplier Code	: H24-3-R2 (KF 840)
Primary purpose	: Hydrotreating naphtha/distillate
Feedstock	: Naphtha/distillate
Catalyst Composition	: Ni/Mo on γ-alumina
Time-on-stream	: 60 days
Temperature	: **not available**
Pressure	: **not available**

6. Naphtha G

Provided by	: Esso Petroleum Canada
Supplier Code	: H24-2, H24-3-R1
Primary purpose	: Hydrotreating
Feedstock	: Wide-cut derived from Athabasca bitumen and also naphtha/distillate
Catalyst Composition	: Ni/Mo on γ-alumina
Time-on-stream	: 100 days for wide-cut feed and 40 days for naphtha/distillate
Temperature	: **not available**
Pressure	: **not available**

7. Gas-oil A

Provided by	: Syncrude Canada Ltd.
Supplier Code	: Xytel Sys # A Canister NM 506
Primary purpose	: S, N removal, saturation of aromatics
Feedstock	: Gas-oil
Catalyst Composition	: Ni/Mo on γ-alumina
Time-on-stream	: 4 weeks
Temperature	: 360-400^{0}C
Pressure	: 9.6-11.0 MPa

8. Gas-oil B

Provided by	: Syncrude Canada Ltd.
Supplier Code	: Xytel Sys # 3
Primary purpose	: S, N removal
Feedstock	: Gas-oil
Catalyst Composition	: Ni/Mo on γ-alumina
Time-on-stream	: 1 year
Temperature	: 360-400 ^{0}C
Pressure	: 9.6-11.0 MPa

9. Gas-oil C

Provided by	: Imperial Oil Ltd.
Supplier Code	: Shell 411
Primary purpose	: HDS, HDN, Hydrogenation
Feedstock	: Heavy coker gas-oil and atmospheric gas-oil in the ratio 7:3
Catalyst Composition	: Ni/Mo on γ-alumina
Time-on-stream	: two years
Temperature	: **not available**
Pressure	: **not available**

10. Bitumen A

Provided by	: Syncrude Canada Ltd.
Supplier Code	: SYN HC-1
Primary purpose	: hydrotreating bitumen
Feedstock	: Athabasca bitumen
Catalyst Composition	: Co/Mo on γ-alumina
Time-on-stream	: 2.5 weeks
Temperature	: 430 ^{0}C
Pressure	: 11.5-14.0 MPa

11. Bitumen B

Provided by	: Syncrude Canada Ltd.
Supplier Code	: SYN HC-2
Primary purpose	: hydrotreating bitumen
Feedstock	: Athabasca bitumen
Catalyst Composition	: Co/Mo on γ-alumina
Time-on-stream	: 25 days
Temperature	: 430 ^{0}C for 2 weeks; 410 ^{0}C for one week
Pressure	: 11.5-14.0 MPa

12. MD-A

Provided by	: Syncrude Canada Ltd.
Supplier Code	: TK 551
Primary purpose	: S, N removal; saturation of olefins and polynuclear aromatics
Feedstock	: Naphtha
Catalyst Composition	: Ni/Mo on γ-alumina
Time-on-stream	: 18 months
Temperature	: **not available**
Pressure	: **not available**

13. MD-B

Provided by	: Syncrude Canada Ltd.
Supplier Code	: HDN-30
Primary purpose	: S, N removal; polyaromatics saturation
Feedstock	: Middle-distillate hydrotreating
Catalyst Composition	: Ni/Mo on γ-alumina
Time-on-stream	: 26 months
Temperature	: 350-450 ^{0}C
Pressure	: 12-20 MPa

14. Silica A

Provided by	: Shell Canada Inc.
Supplier Code	: Shell S-917
Primary purpose	: hydrodemetallization
Feedstock	: Residual feedstock
Catalyst Composition	: Ni/V on silica
Time-on-stream	: **not available**
Temperature	: **not available**
Pressure	: **not available**

15. Silica B

Provided by	: Shell Canada Inc.
Supplier Code	: Shell S-967
Primary purpose	: Demetallization
Feedstock	: Residual feedstock
Catalyst Composition	: Mo on silica
Time-on-stream	: **not available**
Temperature	: **not available**
Pressure	: **not available**

3.1.2 Catalysts from Laboratory Reactors

1. CSTR-1

Provided by	: Syncrude Canada Ltd.
Supplier Code	: KF 840
Primary Purpose	: Hydroprocessing Syncrude Coker Gas-oil
Feedstock	: Syncrude Coker Gas-oil
Catalyst Composition	: Ni-Mo on γ-alumina
Time-on-stream	: 0 hours (Fresh Catalyst)

2. CSTR-2

Provided by	: Criterion Inc.
Supplier Code	: Criterion 411
Primary Purpose	: Upgrading Athabasca Bitumen
Feedstock	: Athabasca Bitumen
Catalyst Composition	: Ni-Mo on γ-alumina
Time-on-stream	: 2 hours
Temperature	: 400 ^{0}C
Pressure	: 13.9 MPa

3. CSTR-3

Provided by	: Criterion Inc.
Supplier Code	: Criterion 411
Primary Purpose	: Upgrading Athabasca Bitumen
Feedstock	: Athabasca Bitumen
Catalyst Composition	: Ni-Mo on γ-alumina
Time-on-stream	: 15.5 hours
Temperature	: 400 ^{0}C
Pressure	: 13.9 MPa

The following data sheet gives the physical properties and elemental analyses of the active metals found on the catalysts. This data is taken from the various data sheets provided by manufacturers.

Table 3.1 Physical Property Data

Catalyst name	metal %	promoter %	size mm	pore vol.cc/g	metal %
Naphtha A	12.9 Mo	3.0 Ni	1.5	0.45	160
Naphtha B	12.9 Mo	3.0 Ni	1.5	0.45	160
Naphtha C	6 MoO_3	2.0 NiO	0.9	0.57	140
Naphtha D	13.2MoO_3	3.5 CoO	1.0	0.82	300
Naphtha E	13.0 Mo	3.2 Ni	1.27	0.438	190
Naphtha F	13.0 Mo	3.2 Ni	1.27	0.438	190
Gas-oil A	27 MoO_3	6.7 NiO	1.5	0.39	220
Gas-oil B	16 MoO_3	2.8 NiO	1.5	0.46	160
Gas-oil C	14.3 Mo	2.6 Ni	1.5	0.43	165
Bitumen A	13 MoO_3	3.5 CoO	0.9	0.82	300
Bitumen B	13 MoO_3	3.5 CoO	0.9	0.82	300
MD-A	14 MoO_3	3.0 NiO	1.59	0.45	180
MD-B	20 MoO_3	5.0 NiO	3.2	0.44	160
Silica A	1.9 V	0.5 Ni	1.9	-----	-----
Silica B	4.0 Mo	45.2	1.9	0.84	259
CSTR-1	13.0 Mo	3.2 Ni	1.27	0.44	190
CSTR-2	14.3 Mo	2.6 Ni	1.5	0.43	165
CSTR-3	14.3 Mo	2.6 Ni	1.5	0.43	165

Table 3.2 Elemental Analysis Data

Catalyst	C	H	N	S	O	Ash	C:H ratio
Naphtha A	8.17	1.08	0.15	7.27	5.76	77.57	7.6
Naphtha B	12.6	0.89	0.13	7.47	5.35	73.55	14.2
Naphtha C	**Not available**						
Naphtha D	5.52	1.45	0.24	6.23	11.4	75.15	3.8
Naphtha E	**Not available**						
Naphtha F							
Gas-oil A	16.3	2.52	0.31	9.63	7.94	63.30	6.5
Gas-oil B	20.3	3.10	0.29	4.38	5.81	66.08	6.6
Gas-oil C	6.30	0.66	0.12	**Not available**			9.6
Bitumen A	15.0	**Not available**					
Bitumen B	10.7	0.84	0.22	**Not available**			12.74
MD-A	5.7	1.22	0.05	**Not available**			4.67
MD-B	**Not available**						
Silica A	7.90	0.42	0.09	**Not available**			18.8
Silica B	7.24	0.91	0.11				7.9

3.2 Preparation of Catalyst Samples

Since the sizes of the catalyst extrudates/rings were of the order of a few mm, it was necessary to hold them together in order to observe under Optical Microscope (OM). This was done by preparing a mold of epoxy resin from 4 parts of epoxy resin to 1 part of epoxy hardener. The catalyst rods were first glued to plasticine in a vertical position and then epoxy resin and hardener mixture was poured into the plastic mold. The plastic mold was first coated with a releasing agent to facilititate the removal of catalyst mold. After 24 hours, the epoxy resin mold was removed from the plastic mold and plasticine was removed from the surface. This procedure was similar to the cold mounting procedure used in coal and coke petrography.

3.2.1 Polishing of Catalyst Samples

To observe the interior of the catalyst pellets, it was necessary to polish off the exterior surface and expose the interior structure. This procedure was done in two steps :

1. Crude polishing : The resin mold, with catalyst rods embedded vertically, was first polished on a duo belt wet surfacer to remove any plasticine and other impurities on the surface. This mold was then consecutively polished on silicon carbide 240 grit, 320 grit, 400 grit, and 600 grit polishing surfaces with cold water as the medium.

2. Final polishing : The resin mold was then fine polished using first a 0.3 μ alumina solution (0.3 μ particle size γ-polishing alumina suspended in distilled water) and then 0.05 μ alumina solution.

Two such samples were prepared for each catalyst, one as a reference and the other to be used in subsequent analyses.

3.3 Microscopic Analysis of the Catalysts

In order to observe the nature of the coke deposits on catalysts, it was necessary to study the interior of the catalyst pellets through various microscopic techniques available in this study. The techniques used were :

1. Optical microscopy

2. Confocal Laser Scanning Microscopy

3. Scanning electron microscopy with energy dispersive X-ray analysis

3.3.1 Optical Microscopy

Optical microscopy examination was carried out in two steps; measurement of reflectance values and measurement of areas of the bright domains. Reflectance microscopy examination was performed by Vincente Munoz at Canada Centre for Mineral and Energy Technology (CANMET), Fuel Processing Laboratory, Devon, Alberta, Canada.

A Carl Zeiss research microscope-photometer with an incident light system was used for the microscopic analysis of the catalysts. A halogen lamp with an average brightness of 1750 cd/cm^2 provided the white light.

Reflectance measurements were done under bright field illumination (polarizer out) polarized light with 600 X magnification at 545 nanometres using an oil immersion objective. The values were obtained from clearly distinguishable features such as dark and bright areas which were observed in photomicrographs. At least 50 reading were obtained from each of the features considered for measurements.

Examination of the fluorescent characteristics of the samples was done using a high pressure mercury lamp with an average brightness of 170,000 cd/cm^2. The selection of the wavelength of the incident beam was accomplished with a combination of filters which provided a range from 450 to 490 nanometres (blue light).

The samples were prepared by the same method described in Section 3.2.

Optical microscopy examination for area measurements was performed in the Mining, Metallurgical and Petroleum Engineering Department of the University of Alberta.

A Carl Zeiss Ultraphot III optical microscope with reflected light system was used. A tungsten light of average brightness 1200 cd/m^2 provided the white light. The microscope was equipped with a Polaroid 4x5 land film holder. Photomicrographs were

taken on Type 55 Positive/Negative Polaroid film with a meter setting of 50 ASA or 18 DIN. The photographs were taken under bright field illumination with non-polarized light at a magnification of 200 X and were of 9 x 11.5 cm. size.

3.3.2 Introduction to Confocal Laser Scanning Microscopy (CLSM)

Two technical problems were encountered during the determination of fluorescence by optical microscopy. One was the difficulty in the determination of the background fluorescence, which did not allow the proper identification and quantification of the emitting microscopic entities. Another problem was the out of focus areas in the field of view at high magnification. This problem was thought to be due to the difficulties in obtaining a flat surface during sample preparation.

These problems could be solved by using confocal laser scanning microscopy, or CLSM. It combines some of the features of optical microscopy and scanning electron microscopy (SEM). Analogous to SEM, the CLSM scans the microscopic entities with a laser beam. The reflected or emitted i.e. fluorescent light from the specimen is detected by photomultipliers, digitized and displayed on a monitor. The CLSM is able to remove out of focus information from the image by means of a spatial filter which consists of an adjustable pinhole (iris) set before the detector. This allows the independent imaging of the structures with height differences on the order of the wavelength of the light source, thus permitting profiles, three-dimensional reconstructions, and quantitative measurements of height.

Preliminary CLSM observations of selected samples were conducted by Vincente Munoz at CANMET, Devon using a Bio-Rad MRC-600 imaging system attached to a Nikon Microphot 2 Optical microscope. The instrument was equipped with a Krypton/Argon mixed-gas laser (15 mW) which could provide lines at 488, 568, and 647 nm. Any of these wavelengths or a combination of these wavelengths could be selected by using suitable filters. The conditions for image acquisition are indicated at the corresponding figure captions.

3.3.3 Scanning Electron Microscopy and Energy Dispersive X-ray Analysis

Scanning Electron microscopy allows the imaging of the topography of a solid surface by use of backscattered or secondary electrons, with a resolution, at present, of better than 5 nm.

When passing through a thin specimen, high energy electrons transfer energy to a inner shell electrons and displace them from their atomic energy level. The outer-shell electrons move in the displaced atomic levels and in the process emit X-ray photons with an energy equal to the energy difference between the excited and final atomic states. The energy of the photon is thus characteristic of the emitting atom. Measurement of this energy on a X-ray spectrum enables identification of the nature of atoms present in the specimen. This is essentially the principle of the energy dispersive X-ray spectometry technique (Delannay, 1984). Combination of this technique with SEM allows the conversion of X-ray energy into electron-hole pairs in a perfectly intrinsic silicon crystal providing higher collection efficiency. The specimen is usually separated from the silicon crystal by a thin beryllium window, allowing the detector to be maintained at liquid nitrogen temperature within a protected vacuum chamber. Owing to the adsorption of low energy X-rays by this window, the domain of EDX analysis is restricted to elements of atomic number $Z \geq 11$ (Delannay, 1984).

3.3.4 Characterization by SEM and EDX-ray Analysis

SEM and EDX-ray analysis photomicrographs were obtained by Ms. Tina Barker of the Mining, Metallurgical and Petroleum Engineering Department at the University of Alberta.

A Hitachi S-2700 Scanning Electron Microscope with a Link eXL Energy Dispersive X-ray Analysis was used in this study. The accelerating voltage was kept at 20 KV. The magnification and the resolution used were changed depending on the size of the coke deposits and type of specimen. The catalyst samples prepared for optical microscopy could also be used in SEM analysis. They were coated with microscopic layer of carbon in

a vacuum evaporator prior to their analysis to make them conductive.

To identify the same field of view through optical as well as electron microscopes, a registration mark was used to fix the location on the surface on the pellet. This was done by fixing a detachable copper foil in the shape of a pointed arrow indicating the same field of view.

CHAPTER 4 : RESULTS

4.1 Introduction to Optical Microscopy Examination of Carbonaceous Materials

The deposits within the catalyst pellets were examined by optical microscopy (OM). Optical microscopy was performed based on several characteristics, as follows : reflectance, isotropic or anisotropic character of the deposits, fluorescence, morphology and color. These characteristics were used to identify and differentiate between the deposits within pellets of spent catalyst.

Since the reflectance of carbonaceous materials increases with aromaticity (Stach *et al.*, 1973; Weinberg and Yen, 1982) the appearance of deposits could be linked to heterogeneous deposition of aromatics. To study this heterogeneity, image analysis of the photomicrographs of the deposits was essential. The first stage was qualitative observation of pellets, followed by quantitative image analysis.

4.2 Qualitative Results of Optical Microscopy

Initial qualitative results from examination of spent catalysts were obtained by Vincente Munoz at the Canada Centre for Mineral and Energy Technology (CANMET) Laboratories in Devon, Alberta. These results were obtained by performing optical microscopic analysis on the following catalysts:

Naphtha A, Naphtha B, MD-A, Bitumen A, CSTR-1, CSTR-2 and CSTR-3.

4.2.1 Reflectance of Naphtha Catalyst Pellets

Figure 4.1 shows a typical view of a Naphtha A catalyst pellet at 300 X magnification under bright field illumination and oil immersion. Carbonaceous deposits are indicated as bright areas (B) which are distributed in a dark matrix (D) formed by deposited organics of low reflectance. Figure 4.2 shows part of Figure 4.1 at 1900 X magnification. This photomicrograph reveals more details of the morphology of bright areas which clearly show inclusions of dark areas within bright areas. The reflectance of deposit marked (B) was 1.61 % compared to 0.75 % for the surrounding dark matrix.

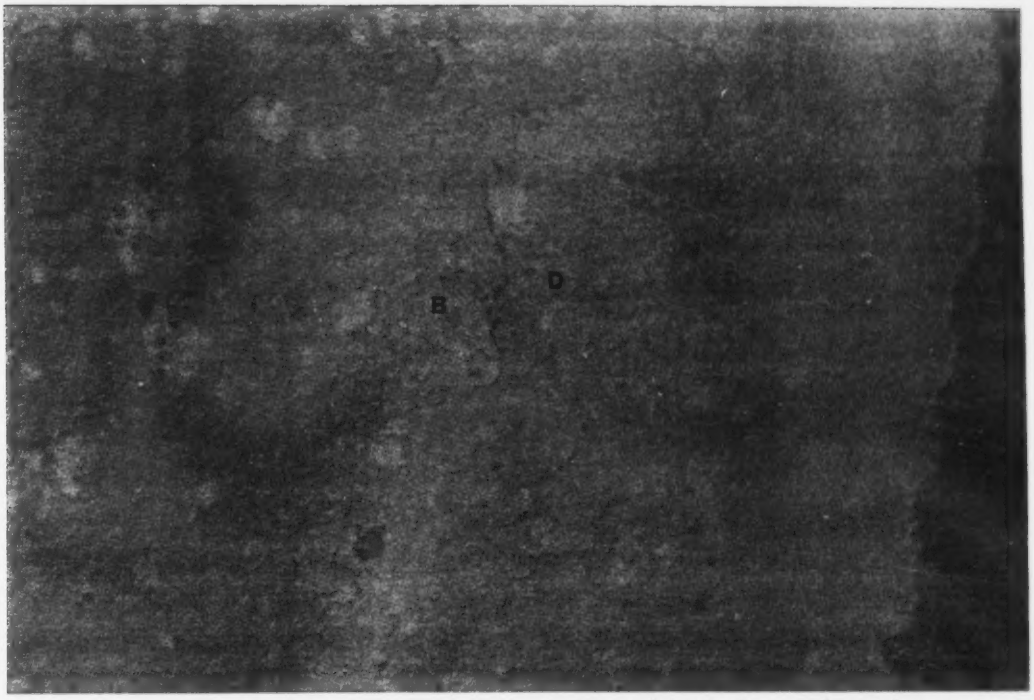

Figure 4.1 : Naphtha A under bright field illumination at 300 X magnification

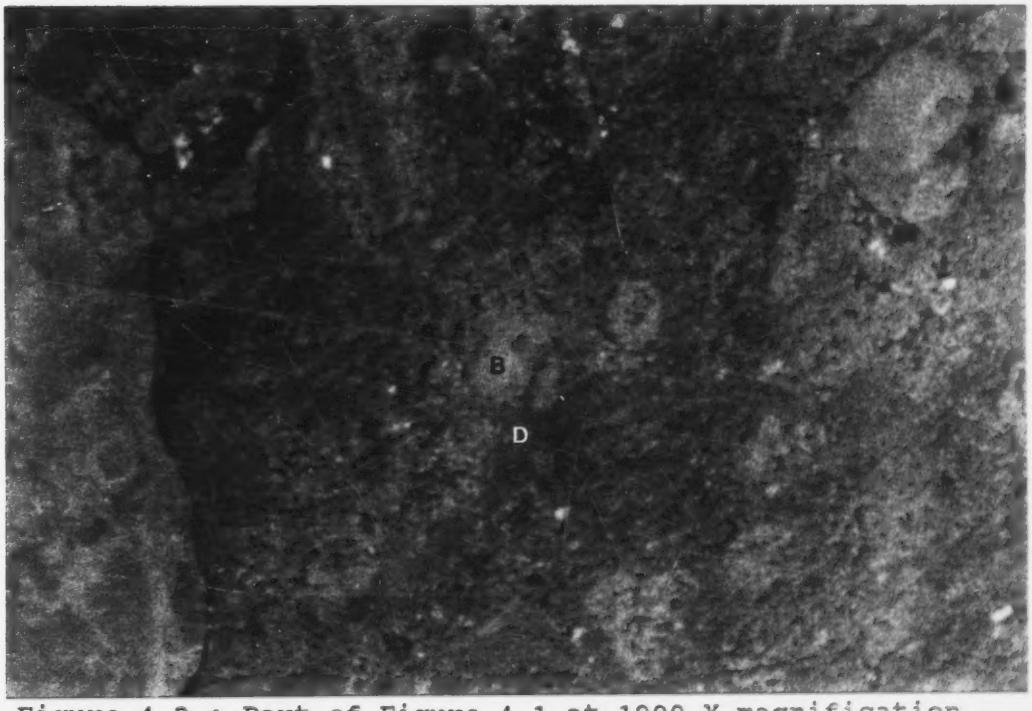

Figure 4.2 : Part of Figure 4.1 at 1900 X magnification

Figure 4.3 shows a typical view of Naphtha B catalyst at 300 X magnification. It shows bright and dark areas similar to Naphtha A catalyst. The bright areas in Naphtha B have higher reflectance than their counterparts in Naphtha A; the reflectance of bright area (B) is 1.82 % and that of the dark area (D) is 0.75 %.

Figure 4.4 shows the same field of observation as in Figure 4.1 for Naphtha A catalyst, but under cross-polarized light. Figure 4.4 shows that many of the high-reflectance components also possess anisotropic characteristics. Naphtha B catalyst did not show any anisotropic character under cross-polarized light.

4.2.2 Reflectance of Middle Distillate Catalyst Pellets

Figure 4.5 shows an optical micrograph of MD-A under polarized light, oil immersion and at 600 X magnification. Bright components could be seen throughout the dark matrix.

4.2.3 Optical Microscopy of Bitumen Catalyst Pellets

Figure 4.6 shows Bitumen A catalyst sample at 220 X magnification. The photomicrograph reveals bright inclusions in the dark matrix.

Figure 4.7 shows a CSTR-1 sample under partially cross-polarized light. The micrograph depicts the interior areas of low reflectance and the unpolished outer areas which produced scattering of the incident light.

Figure 4.8 shows a typical view of CSTR-2 under polarized light, oil immersion at 220 X magnification. This photomicrograph reveals the concentration of dark components (d) at the edge of the polished extrudate. Organic agglomerates (a) were attached to the external surface of the extrudate. Figures 4.9 and 4.10 show the area marked with an arrow in Figure 4.8 at a much higher magnification of 1650 X. From Figure 4.9, it can be seen that there is higher concentration of inorganics in the outer areas of polished surface indicating deposition of metals. Figure 4.10 reveals the presence of organic agglomerates attached to the inorganic outer areas of the extrudate.

Figure 4.11 shows CSTR-3 under polarized light, oil immersion at 1650 X. The

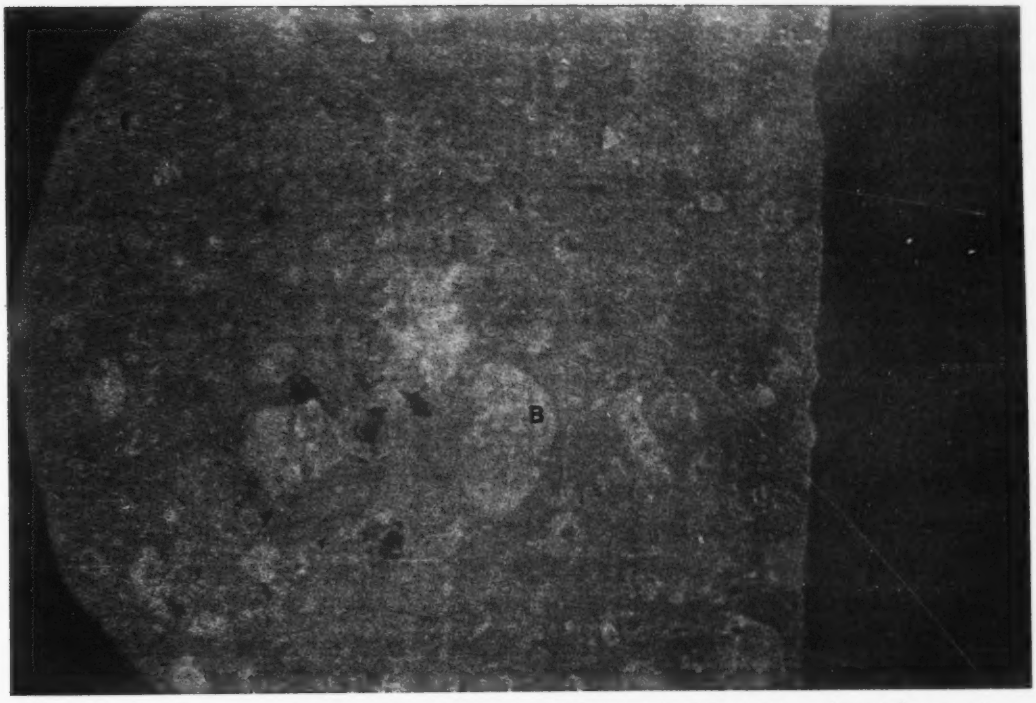

Figure 4.3 : Naphtha B under bright field illumination at 300 X magnification

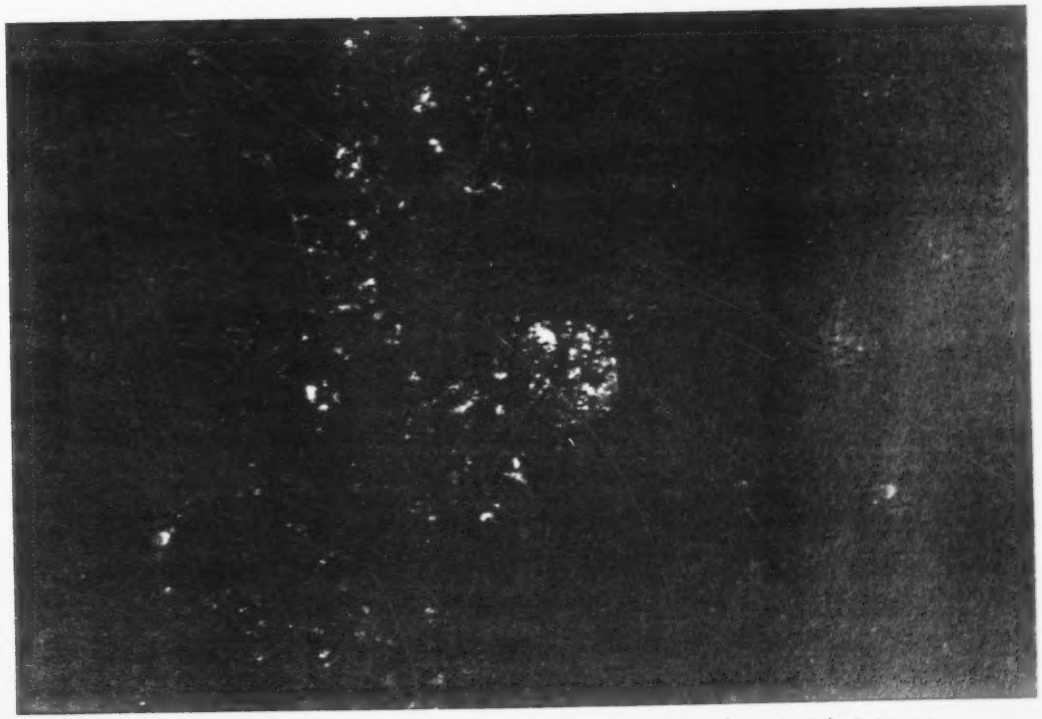

Figure 4.4 : Naphtha A under cross-polarized light at 300 X magnification

Figure 4.5 : MD-A under polarized light, oil immersion at 600 X magnification

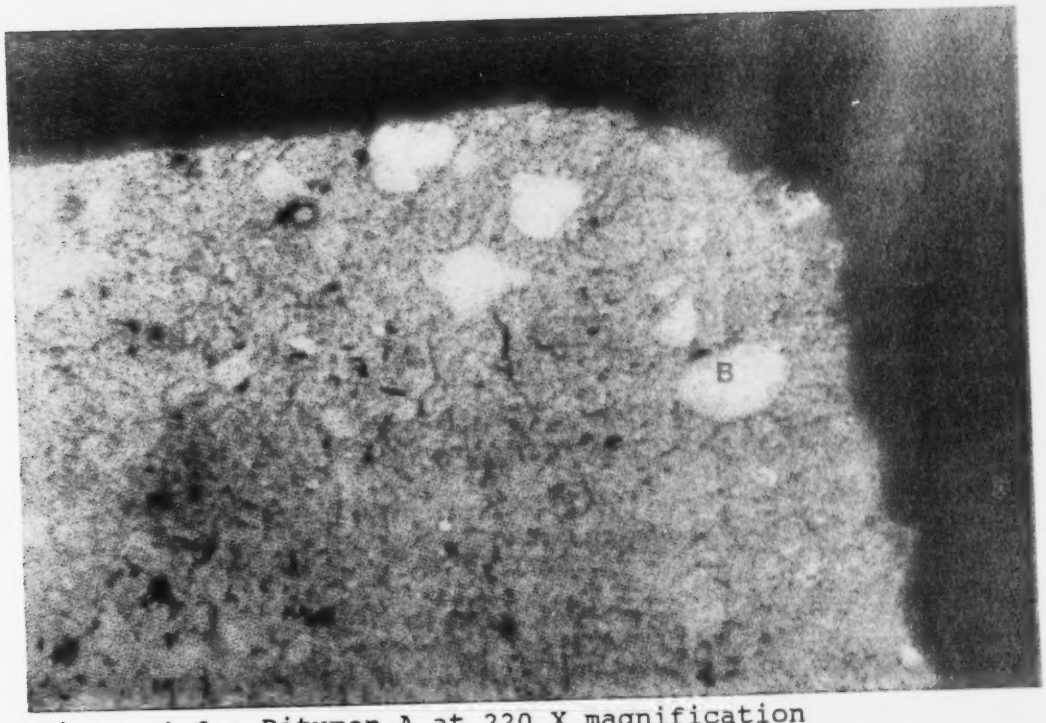

Figure 4.6 : Bitumen A at 220 X magnification

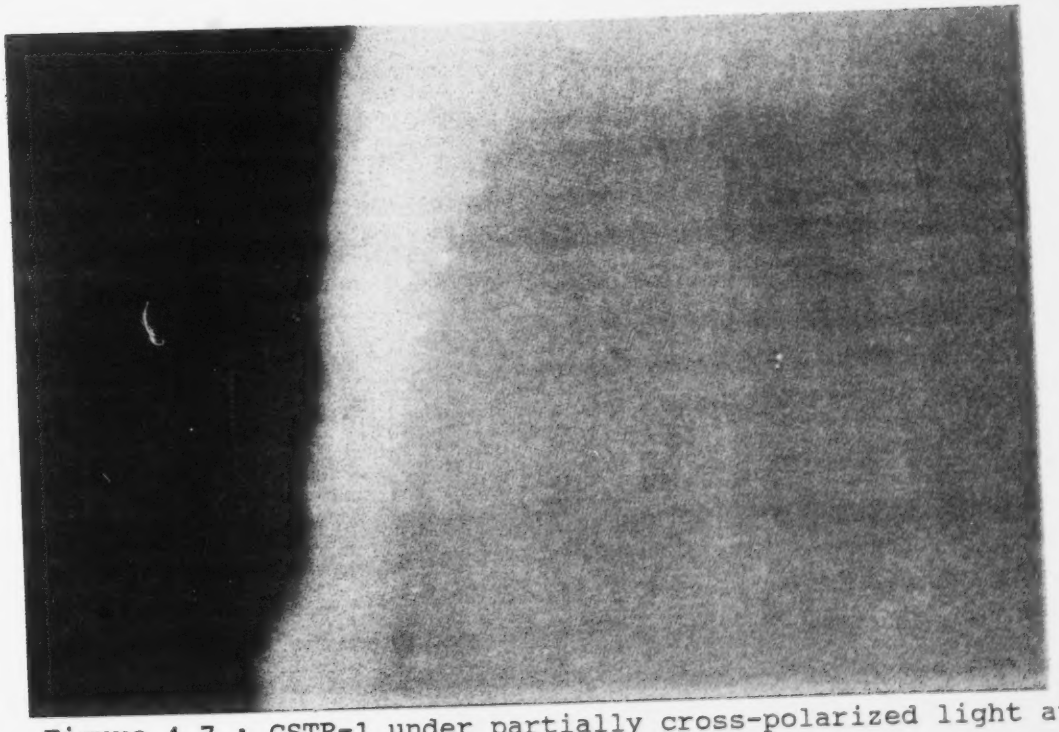

Figure 4.7 : CSTR-1 under partially cross-polarized light at 220 X magnification

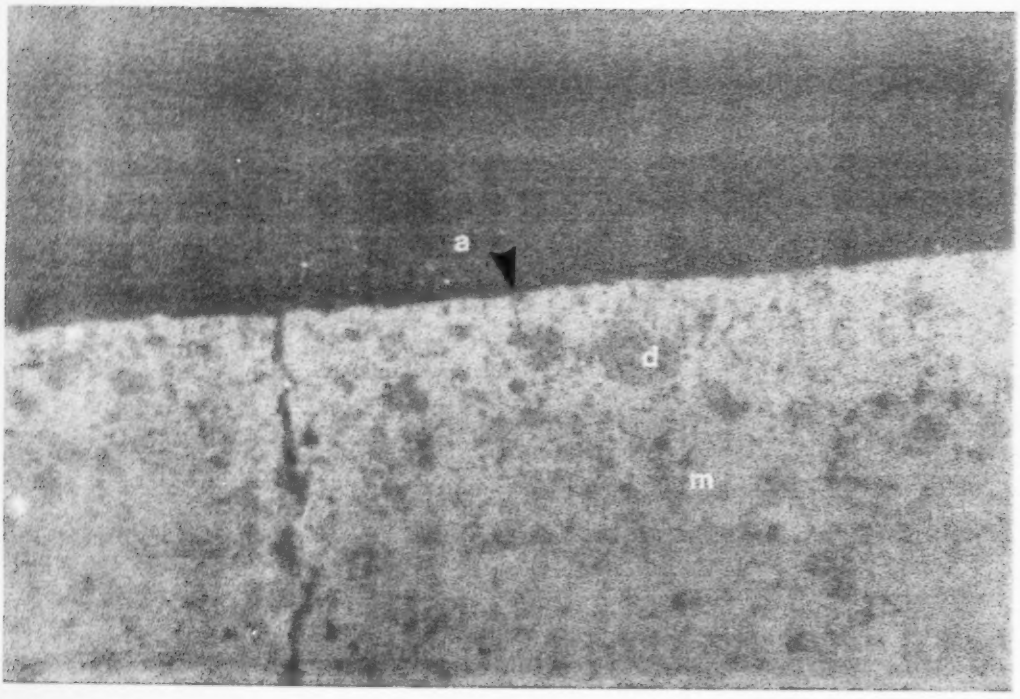

Figure 4.8 : CSTR-2 under polarized light, oil immersion at 220 X magnification

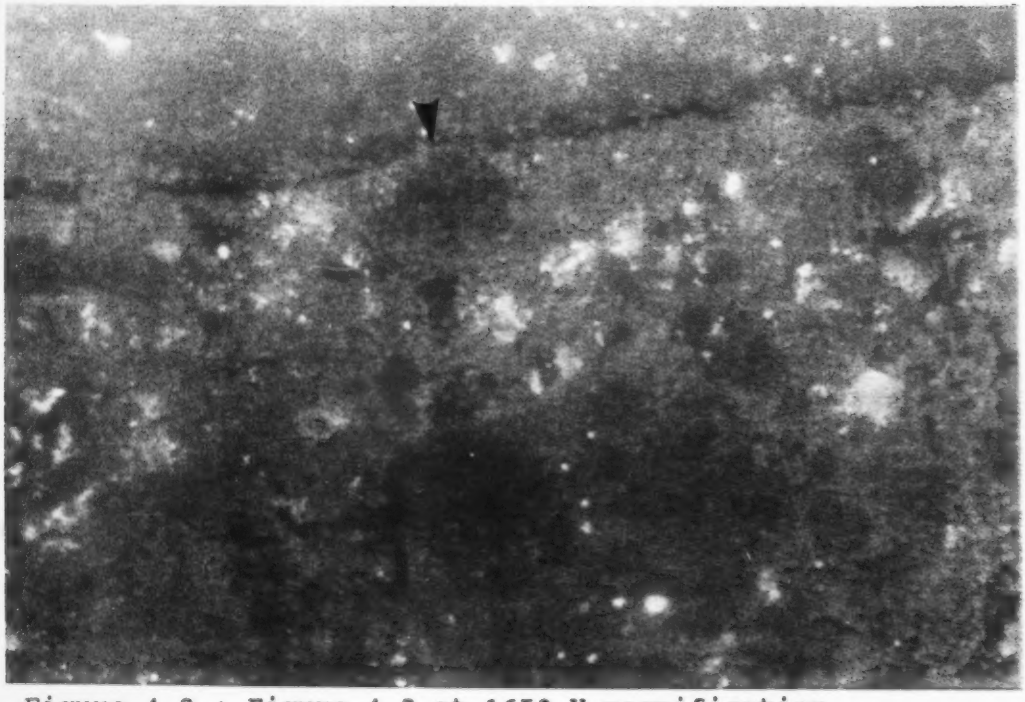

Figure 4.9 : Figure 4.8 at 1650 X magnification

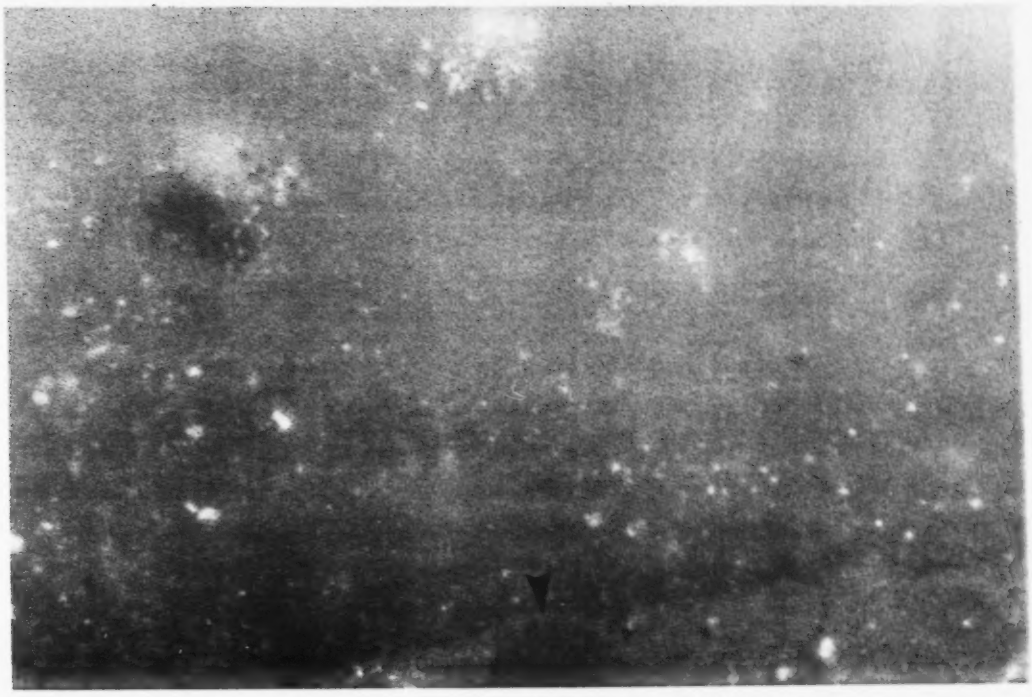

Figure 4.10 : Figure 4.8 at 1650 X magnification

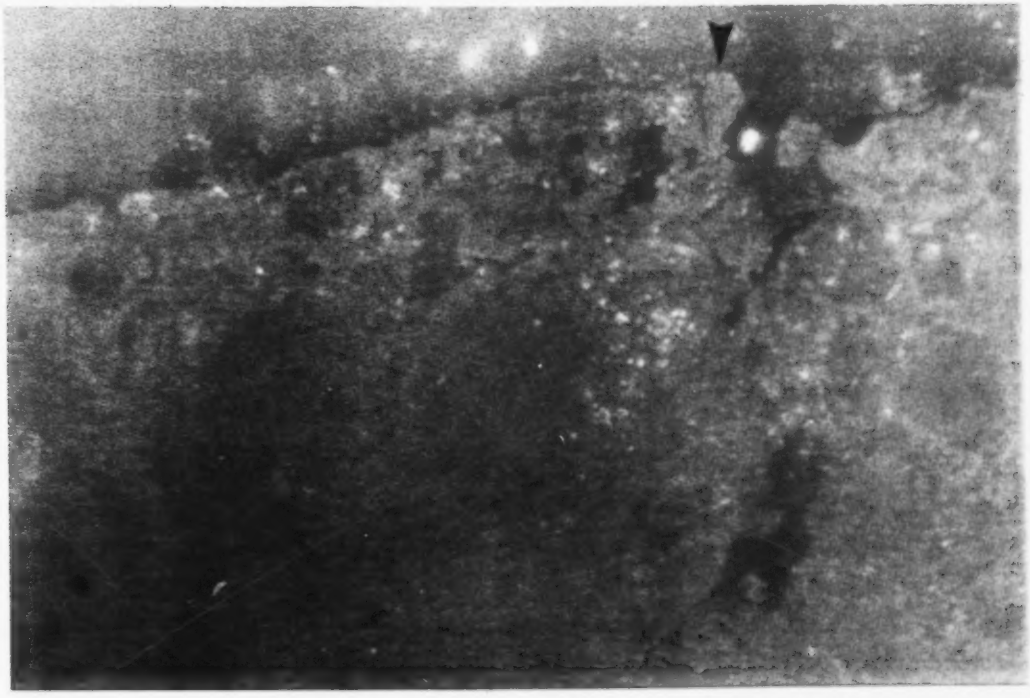

Figure 4.11 : CSTR-3 under polarized light, oil immersion at 1650 X magnification

amount of organic agglomerates attached to outer edge was less than that in the case of the CSTR-2 catalyst.

4.2.4 Fluorescence Microscopy of Catalyst Pellets

Figure 4.12 shows a view at 420 X of a Naphtha A catalyst pellet with bright areas included in a dark matrix. Figure 4.13 shows the same field of view where imaging was done using a blue light source, with a filter, to observe the fluorescence characteristics of the low reflectance matrix. Clearly the high reflectance areas were not fluorescent but the dark matrix shows a yellow fluorescence of different intensity through the field of view. None of the Naphtha B catalyst pellets analyzed showed fluorescence.

Figure 4.14 shows a typical dark area in case of CSTR-2 under cross-polarized light. Figure 4.15 shows that the same dark component exhibits fluorescence under blue light (450-490 nm). None of the other catalysts examined showed fluorescent properties.

The fluorescent properties of the deposits found in Naphtha A and CSTR-2 indicate that they were composed of organics with a highly conjugated double bond system constituted by aromatic and aliphatic fractions. These compounds would possess higher H-content compared to the non fluorescent pellets. Analysis of the extracts from the same spent catalysts indicated that Naphtha A contained more extractable N-rich organic material (Choi and Gray, 1988) and also the carbon deposits were less aromatic on average as determined by ^{13}C-NMR (Egiebor *et al.*, 1989).

4.2.5 Qualitative Results of CLSM Examination

Figure 4.16 shows the CLSM photograph of the CSTR-1 catalyst sample, where 64 optical sections are shown. Each section was 1 μm in thickness. The 3-D effect can be perceived using the red/green glasses provided in the back pocket of this thesis.

Figure 4.17 shows a CLSM photograph of the CSTR-3 with a pseudocolor presentation where 38 optical sections each with a step size of 0.8 μm were taken. The 3-D structure of the deposited organic agglomerates can be perceived using the red/green glasses.

Figure 4.12 : Naphtha A at 420 X magnification

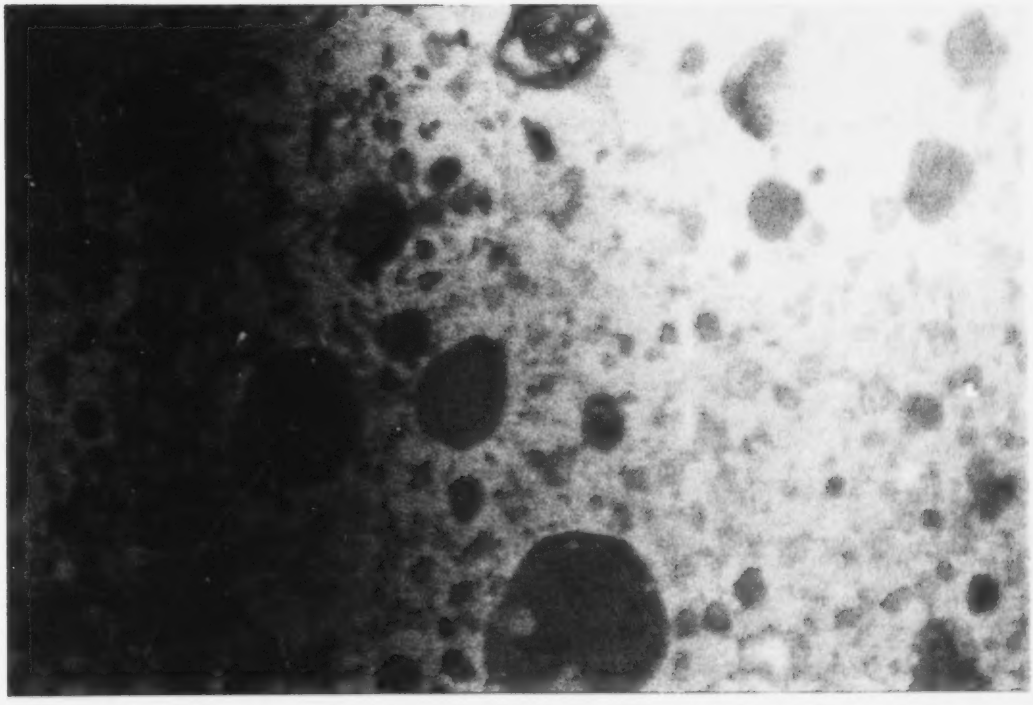

Figure 4.13 : Figure 4.12 under a blue light source

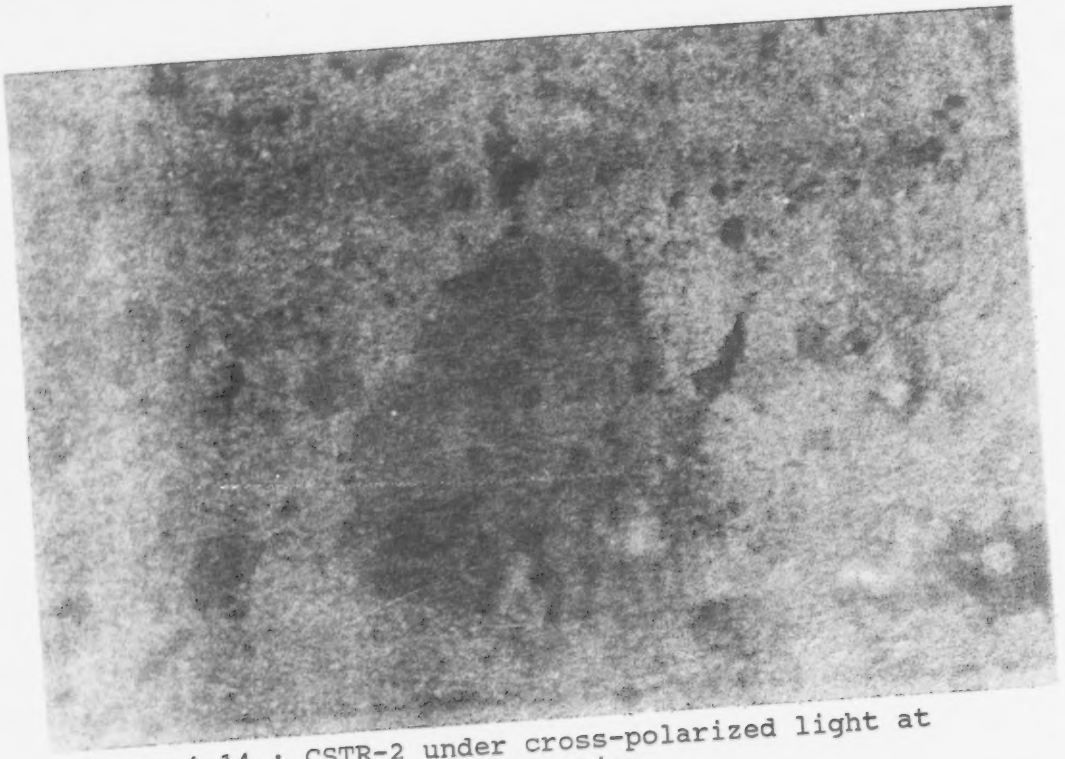

Figure 4.14 : CSTR-2 under cross-polarized light at 1900 X magnification

Figure 4.15 : Figure 4.14 under blue light (450-490 nm)

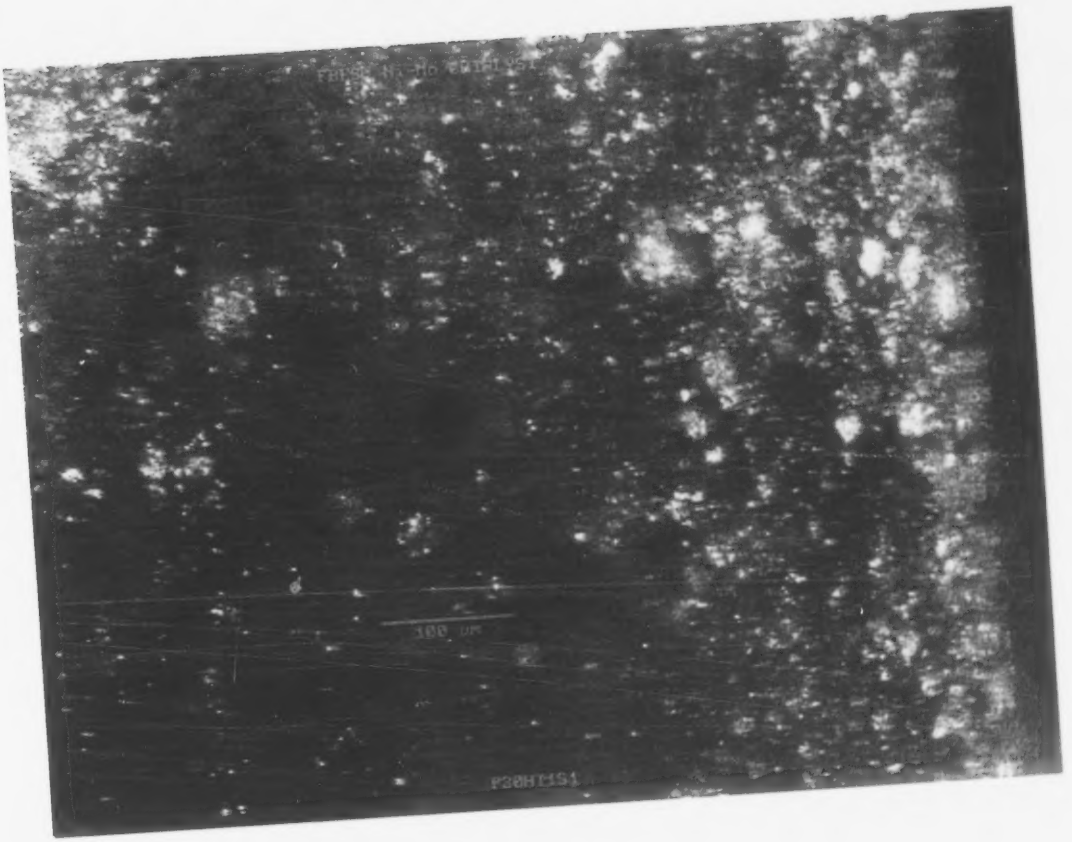

Figure 4.16 CLSM Photograph of CSTR-1 with 64 optical sections at 300 X magnification

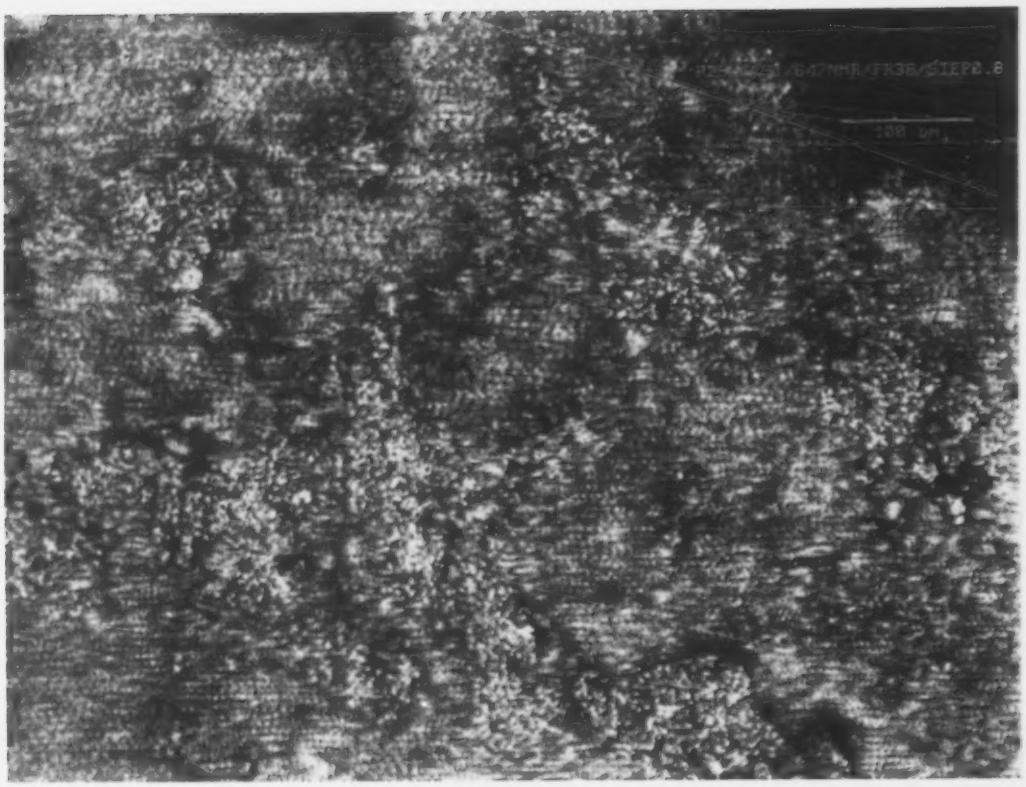

Figure 4.17 CLSM Photograph of CSTR-3 with 38 optical sections at 220 X magnification

4.3 Quantitative Results of Optical Microscopy

In order to characterize the reflectance distribution and the size and distance distribution of reflectance areas, quantitative measurements of these bright regions were made. The commercial spent catalysts which showed these bright regions are listed in Table 4.1.

4.3.1 Reflectance Measurements

The mean random reflectance values are presented in Table 4.2. The Naphtha A catalyst had an overall reflectance of 0.64 % compared to 0.87 % in the Naphtha B catalyst. These values included both the dark and bright areas found in the catalyst pellets. The bright and dark areas of the Naphtha A catalyst had mean reflectance values of 0.86 % and 0.46 % respectively and the corresponding features in the Naphtha B catalyst had values of 1.18 % and 0.55 % respectively. These results demonstrate that the carbonaceous deposits in the Naphtha A catalyst were less aromatic than those found in the Naphtha B catalyst in agreement with ^{13}C-NMR measurements which average over the entire pellet volume (Egiebor *et al.*, 1989). The histograms of the reflectance distributions are presented in Figures 4.18 and 4.19.

Table 4.3 gives the reflectance values in case of CSTR-1, CSTR-2 and CSTR-3 catalyst samples. Table 4.4 gives the reflectance values in case of MD-A and Bitumen A catalysts.

Table 4.1 Commercial Catalysts Showing Bright Regions

Catalyst	Number of Bright Regions
Naphtha A	105
Naphtha B	130
Naphtha C	No bright regions
Naphtha D	No bright regions
Naphtha E	No bright regions
Naphtha F	No bright regions
Gas-oil A	23
Gas-oil B	No bright regions
Gas-oil C	65
Bitumen A	No bright regions
Bitumen B	No bright regions
MD-A	60
MD-B	No bright regions
MD-C	No bright regions
Silica A	No bright regions
Silica B	No bright regions

Table 4.2 Mean Random Reflectance Values for Naphtha A and Naphtha B

Sample	Naphtha A			Naphtha B		
	Bright area	Dark area	Over-all	Bright area	Dark area	Over - all
Mean Random Reflectance	0.86	0.46	**0.64**	1.18	0.55	**0.87**
Sample Standard Variation	0.33	0.20	0.33	0.35	0.20	0.42
Coeffcient of Variation	38.37	43.4	51.56	29.66	36.36	48.2
Number of Observations	54	68	122	54	54	108
Standard Deviation of Mean	0.045	0.02	0.030	0.048	0.027	0.04

Mean Random Reflectance $(\underline{x}) = \dfrac{\sum_{i=1}^{n} x_i}{n}$

Sample Standard Variation $(s) = \sqrt{\dfrac{\sum_{i=1}^{n} (x_i - \underline{x})}{n-1}}$

Coefficient of Variation $(CV) = \dfrac{s}{\underline{x}} \cdot 100$

Standard Deviation of Mean $= \dfrac{s}{\sqrt{n}}$

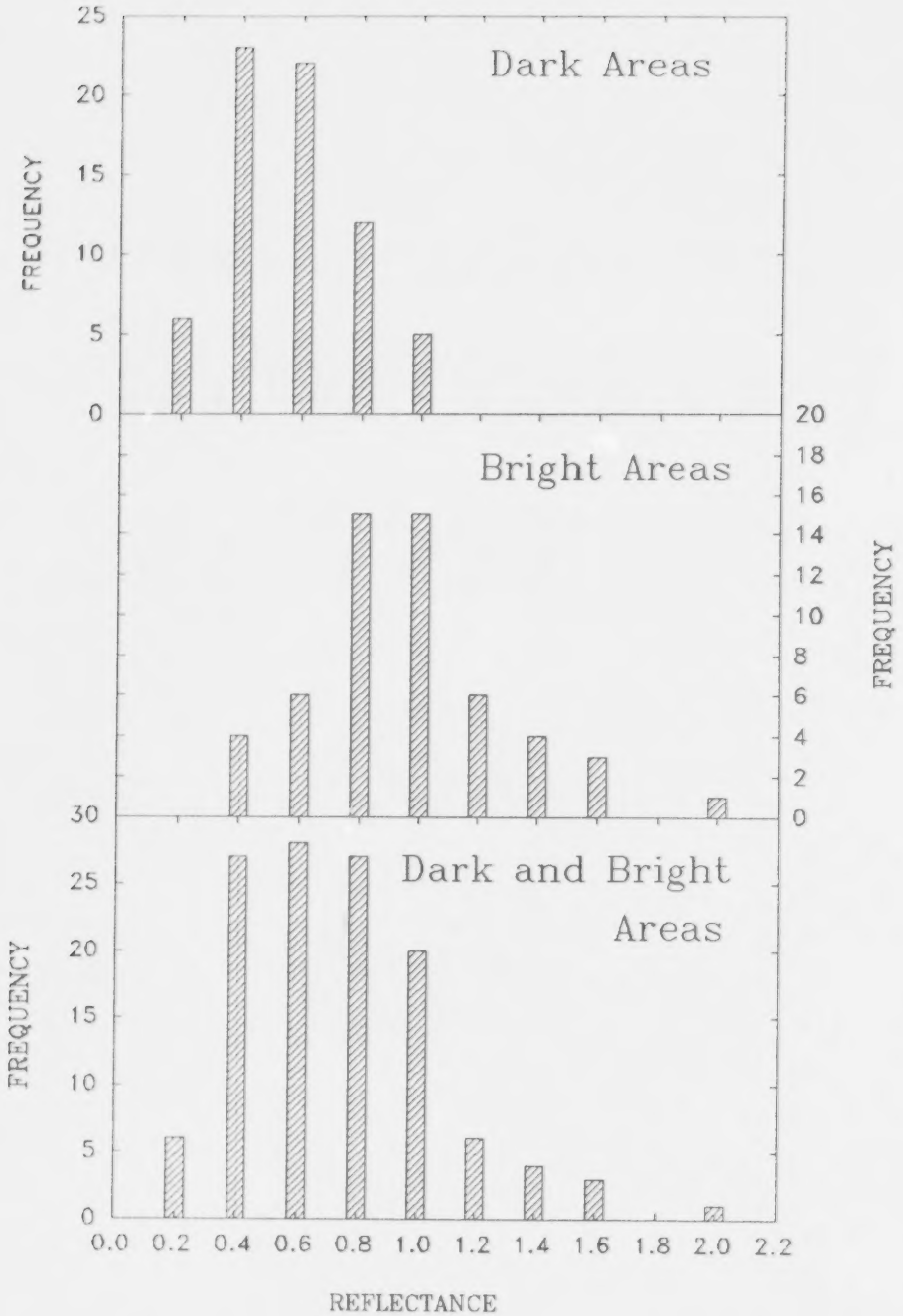

Figure 4.18 : Reflectance Histograms for Naphtha A

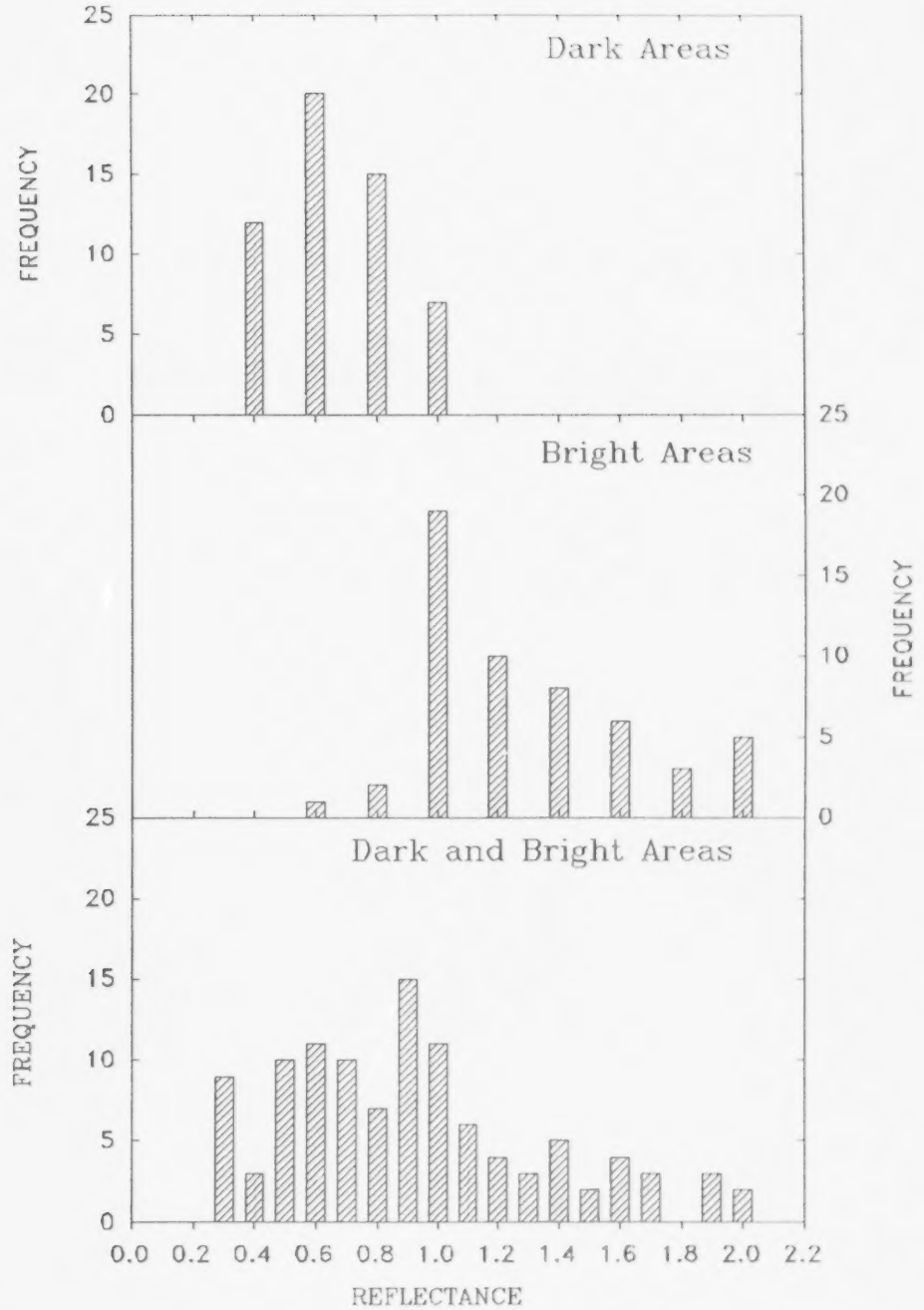

Figure 4.19 : Reflectance Histograms for Naphtha B

Table 4.3 Statistical data of Reflectance Measurements for the Laboratory Spent Catalysts.

DATA	CSTR-1	CSTR-2		CSTR-3	
		Outer area	Inner area	Outer area	Inner area
Data points (*n*)	95	50	50	50	50
Minimum Value	0.07	0.26	0.20	0.32	0.27
Maximum Value	0.33	1.51	0.49	1.64	0.76
Mean Value ($\underline{x}$)	**0.25**	**0.58**	**0.35**	**0.64**	**0.57**
Standard Deviation (s)	0.04	0.24	0.06	0.25	0.10
Coefficient . of Variation $\left[(s/\underline{x})\cdot 100\right]$	16.27	42.46	16.86	39.0	18.34
Standard. Error of Mean ($s/\sqrt{n}$)	0.01	0.07	0.02	0.07	0.03

Table 4.4 Statistical Data of the Reflectance Measurements of the Commercially Spent Catalysts

DATA	MD-A		Bitumen A	
	Outer area	Inner area	Outer area	Inner area
Data Points	50	50	50	50
Minimum Value	0.29	0.30	0.63	0.54
Maximum Value	1.03	0.67	2.57	1.87
Mean Value	**0.56**	**0.46**	**1.59**	**1.12**
Standard Deviation	0.16	0.08	0.49	0.38
Coefficient of Variation	28.60	17.32	30.98	33.60
Standard Error of the Mean	0.04	0.02	0.14	0.10

4.3.2 Area Measurements of Bright Spots

The ratio of the area of the bright spots to the total exposed cross-section was calculated from measurements of five randomly oriented photomicrographs of different pellets of each catalyst type that contained bright regions. The total area occupied by the bright spots in the five photographs, divided by the total imaged area, gave area ratio of bright spots for that particular catalyst sample. Table 4.5 gives the area ratios for the catalysts analyzed. To calculate the average area of bright spots in a catalyst sample, the total area of the bright regions in five micrographs were added and this sum was divided by total number of bright spots. Table 4.5 gives the average areas for the catalysts analyzed. The bright spots in Naphtha B had the highest average area as well as highest area ratio, followed by Naphtha A and Gas-oil C respectively.

It should be noted that in area and size measurements the minimum size of the bright domains that could be seen depends upon the maximum resolution of the optical microscope. It is likely that some of the bright domains had sizes below the minimum size that could be observed with the optical microscope and hence those bright domains were not resolved and were not visible with a clear distinction. In quantitative size measurements, the lower limit of detection with the optical microscope used in this study was 3.1×10^{-6} m.

4.3.3 Area Distribution Measurements

To characterize the range of the areas of the bright spots, the area distribution of these spots was calculated. Equally spaced area ranges were used for all the catalyst samples and then the frequency of the distribution was calculated. These data were then plotted in the form of a bar chart showing number fraction of bright spots vs. the area range. These histograms are given in Figures 4.20, 4.21, 4.22, 4.23, and 4.24 for Naphtha A, Naphtha B, MD-A, Gas-oil A and Gas-oil C respectively. The area and frequency distribution data are given in Appendix I. The distribution of areas in all the catalysts analyzed were different. Naphtha A and Naphtha B showed roughly a binomial

Table 4.5 Area Ratios and Average Areas of Bright Spots

Catalyst	Area Ratio	Average area, m^2
Naphtha A	0.0485	6.0×10^{-10}
Naphtha B	0.0685	5.3×10^{-10}
MD-A	0.0162	6.44×10^{-10}
Gas-oil A	0.007	5.15×10^{-10}
Gas-oil C	0.02	4.68×10^{-10}

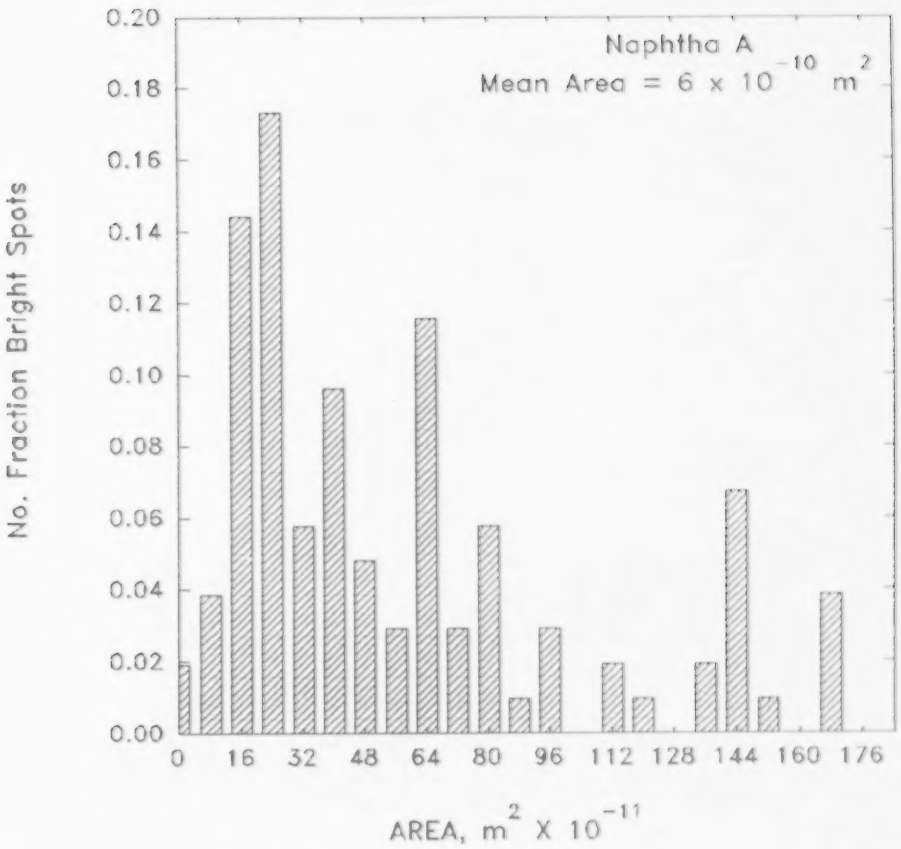

Figure 4.20 : Number Fraction of Bright spots vs. Area range histogram for Naphtha A

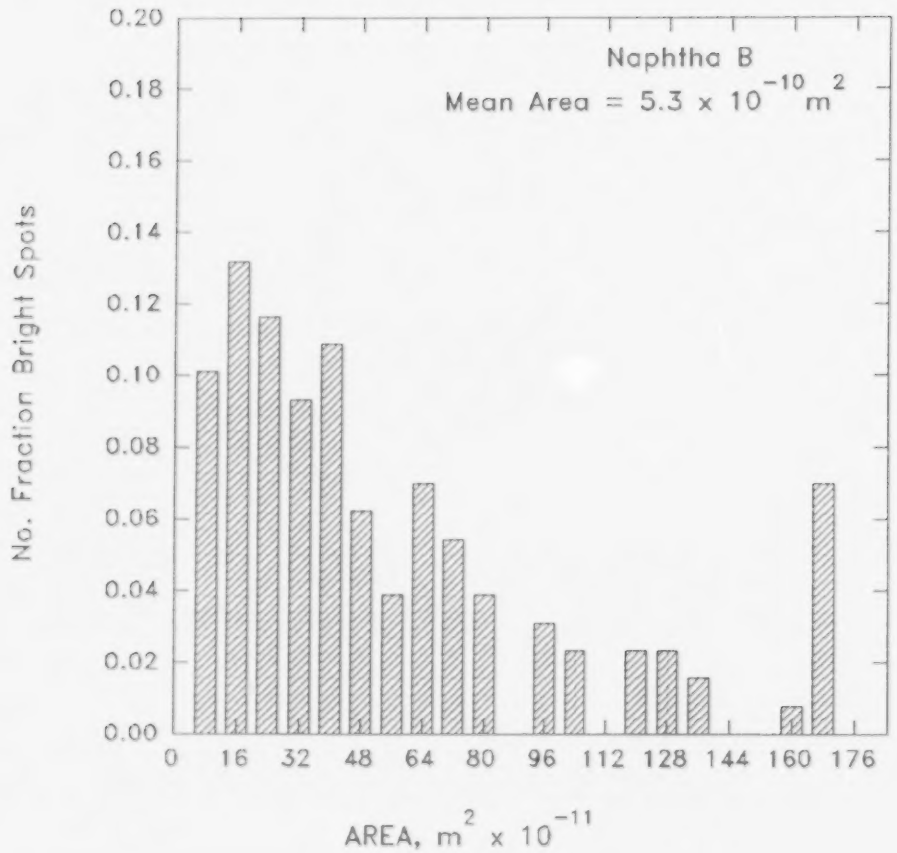

Figure 4.21 : Number Fraction of Bright spots vs. Area range histogram for Naphtha B

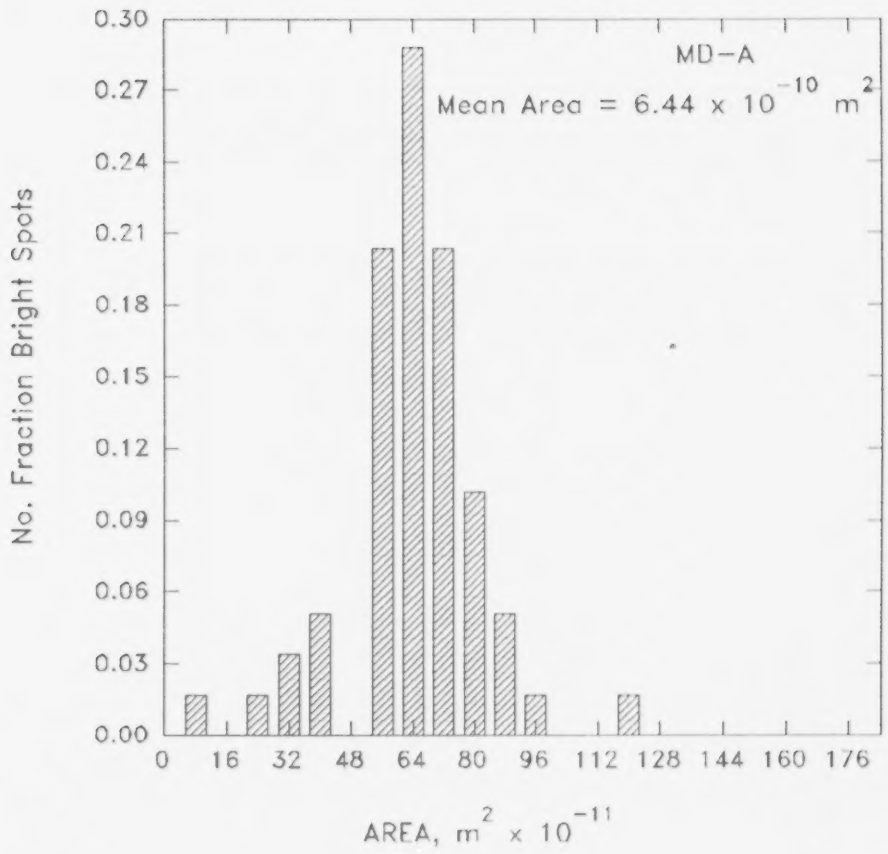

Figure 4.22 : Number Fraction of Bright spots vs. Area range histogram for MD−A

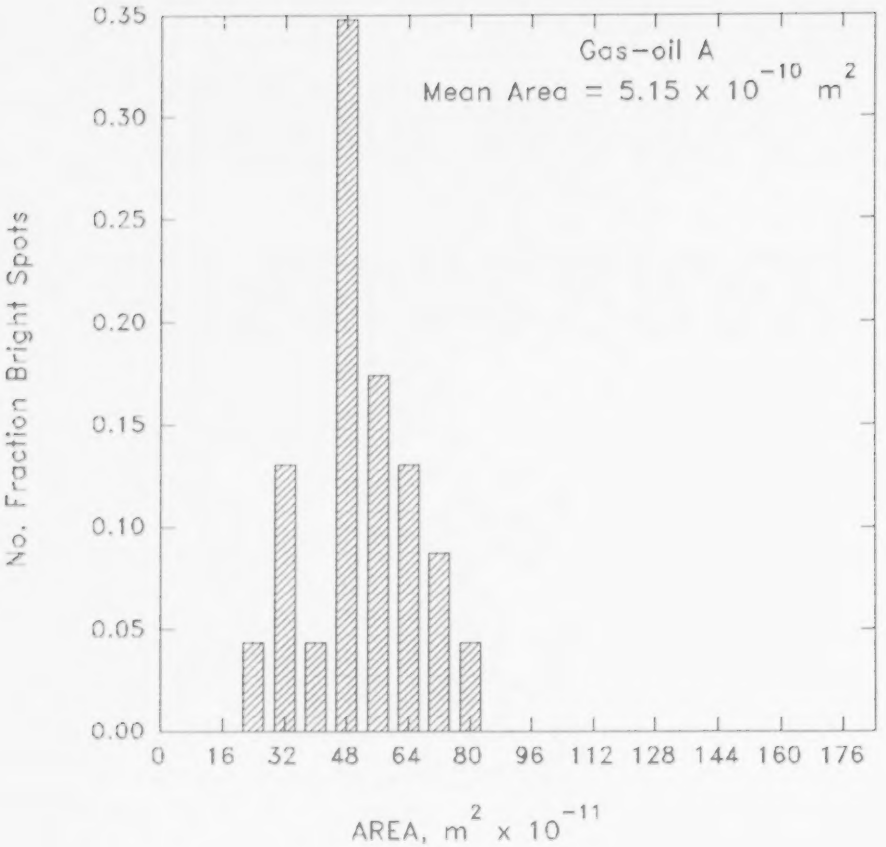

Figure 4.23 : Number Fraction of Bright spots vs. Area range histogram for Gas–oil A

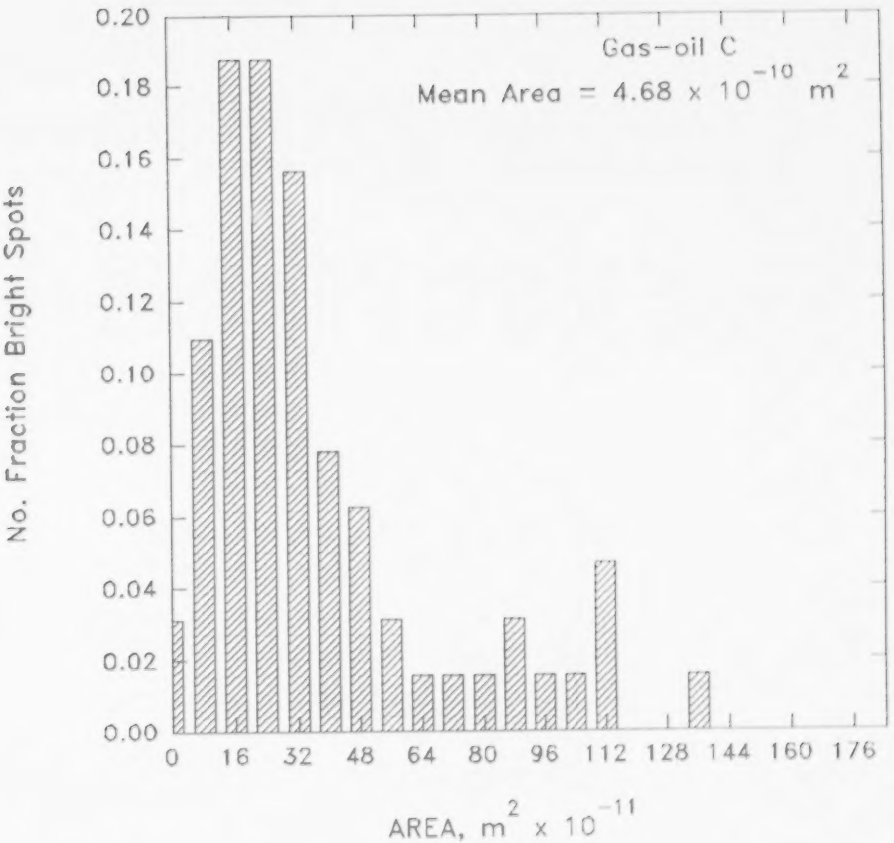

Figure 4.24 : Number Fraction of Bright spots vs. Area range histogram for Gas–oil C

distribution with mean areas of approximately 60 x 10^{-11} m^2, whereas the distribution in Gas-oil C approximated a γ-distribution with a mean area of approximately 46.8 x 10^{-11} m^2.

4.3.4 Distance Distribution Measurements

In the case of MD-A and Gas-oil A, the bright spots were found to be heterogeneously distributed on the catalyst surface. To study this phenomenon further, the distance distribution of these bright spots was measured in a similar fashion as the area distribution. Photomicrographs of the pellet cross-sections were obtained by traversing in the vertical direction. MD-A pellet required three cross-section photographs and Gas-oil C required four of them at the same magnification of 200 X. By joining these photographs together and eliminating any superposition, the distance of the bright spots could be measured from the centre of the catalyst pellet. The frequency and distance distribution data are given in Appendix I. Figure 4.25 gives the histograms of distance distribution. To eliminate any differences in the radii of the catalyst pellets, the histograms were plotted with a non-dimensional distance (distance of a bright spot divided by the radius of that catalyst pellet). The bright spots were observed more frequently near the periphery of the catalyst pellet in both the cases.

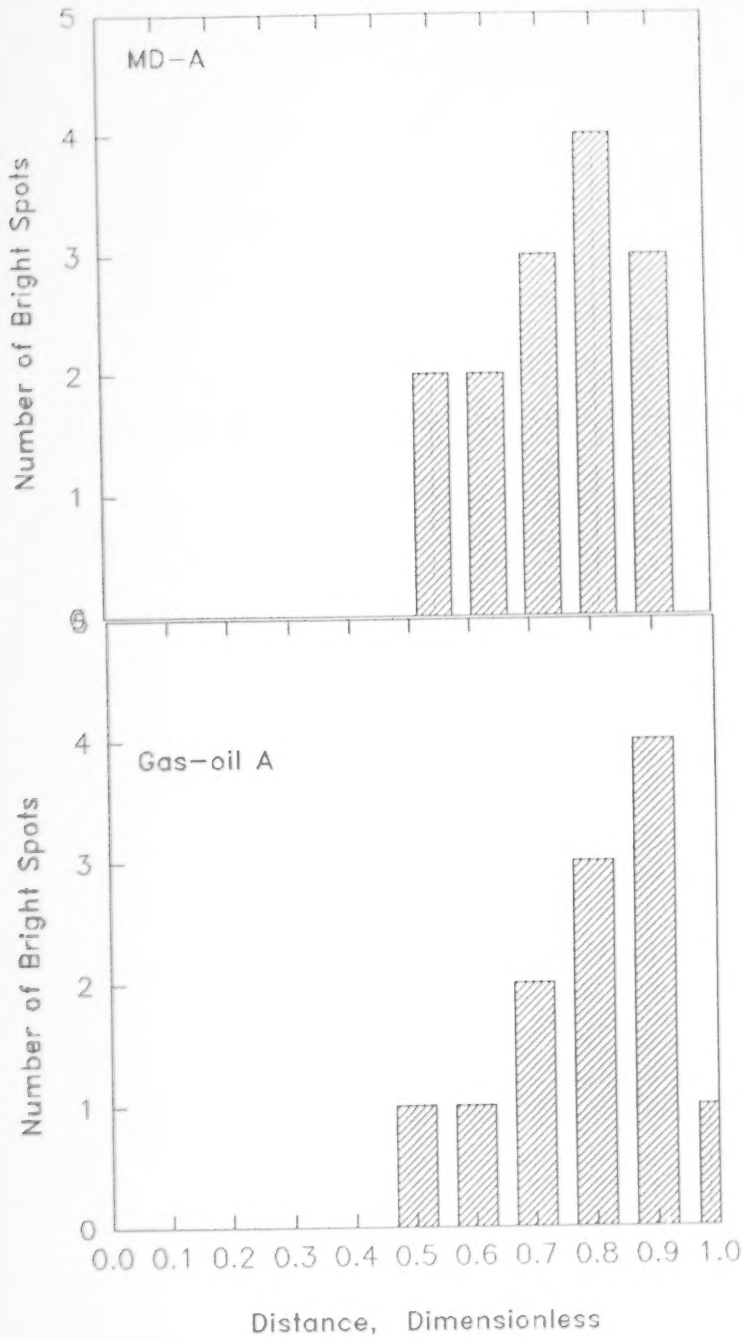

Figure 4.25 : Number Fraction of Bright spots vs. Dimensionless Distance histogram for MD-A and Gas-oil C

4.4 Scanning Electron Microscopy and Energy Dispersive X-ray Analysis of Catalyst Pellets

To understand the nature and origin of the bright spots observed on distillate catalysts, scanning electron microscopy (SEM) and energy dispersive X-ray analysis was performed on three catalyst samples viz., a silica supported catalyst (Silica A), a catalyst for bitumen hydrocracking (Bitumen A), and a catalyst for naphtha hydrotreating (Naphtha A). To get a measure of the heterogeneities in the distribution of metals on the exposed surface of the catalyst, Energy Dispersive X-ray Analysis (EDX analysis) was used. The quantitative results of these experiments are presented below.

4.4.1 SEM Elemental Analysis by EDX for Naphtha A

Various regions having a distinct boundary were observed in SEM analysis. The same type of distinguishable regions were observed under the optical microscope for this catalyst sample. These regions appeared to be distributed uniformly over the surface. Table 4.6 gives the concentrations of selected metals on the surface. To understand the distribution of metals in these regions EDX traversing was used. The incident beam was moved along in one direction in these domains and the peripheral dark matrix. This method was found to be more successful than the conventional EDX mapping technique due to low concentrations of metals. Figure 4.26 shows the EDX traverses for Naphtha A.

It can be seen that there was no appreciable variation in P concentration on the surface. However, Ni concentration increased substantially from dark matrix to the bright circular area. These findings were confirmed by EDX traverses of these distinct regions and the peripheral dark matrix (Figure 4.26).

4.4.2 SEM Elemental Analysis by EDX for Bitumen A

SEM elemental analysis did not show any distinct rounded domains. However, there appeared to be three areas which had grey levels significantly higher than the rest of the matrix. Table 4.7 shows the concentration of selected metals in these areas as well as a general analysis. Figure 4.27 shows the results of EDX traverses of the distinctly different

Table 4.6 Results of SEM analysis for Naphtha A

Region analyzed	S %	P %	Ni %
General analysis	36.96	8.96	3.41
Bright Circular Area	40.72	5.82	3.19
Dark matrix	29.39	5.78	1.51

Table 4.7 Results of SEM analysis for Bitumen A

Region analyzed	S %	Ca %	V %
General analysis	30.32	0.221	17.33
Dark region	30.15	0.208	20.88
Bright region 1	32.15	0.34	22.83
Bright region 2	31.52	1.63	20.24
Bright region 3	30.23	3.87	19.03

Table 4.8 Results of SEM analysis for Silica A

Region analyzed	S %	Ca %	V %
General Analysis	10.62	5.18	1.27
Dark Region	3.82	1.08	0.831
Intermediate Grey Region	8.39	2.46	0.682
Bright Region	11.05	6.96	0.417

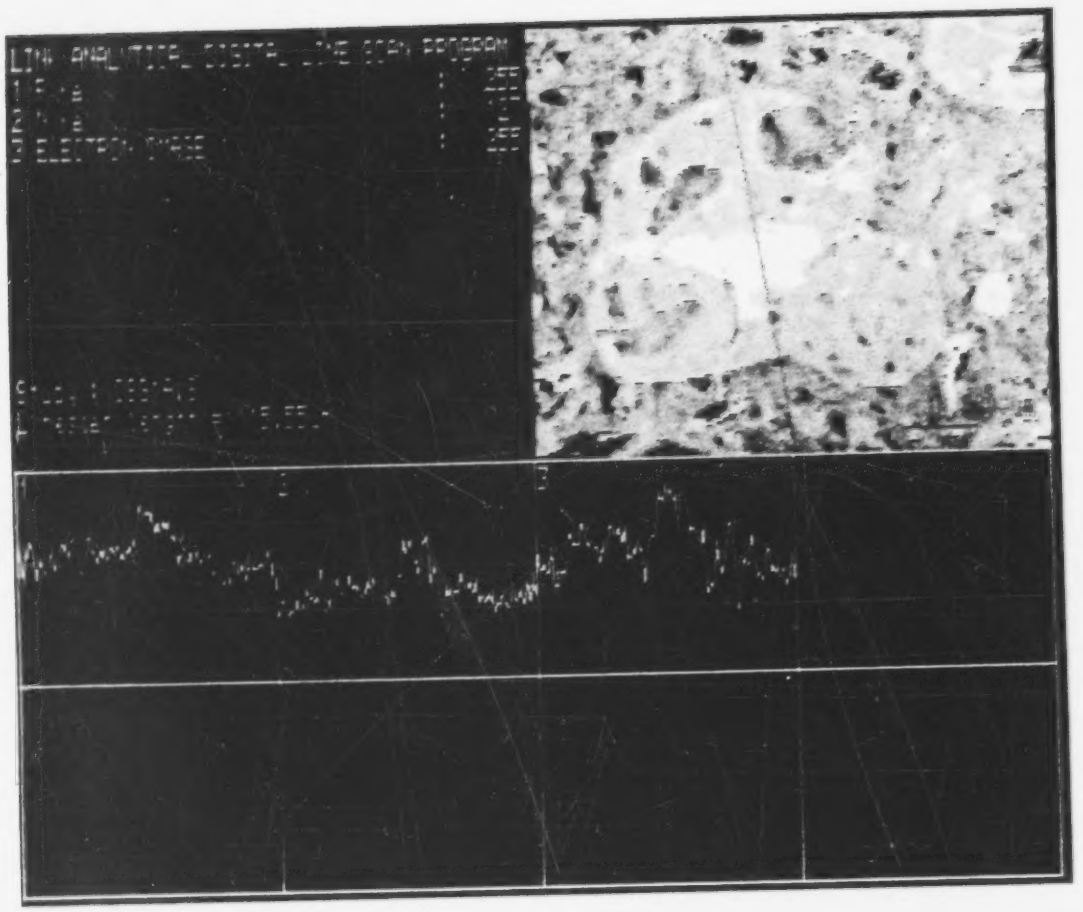

Figure 4.26 : EDX Traverses for Naphtha A

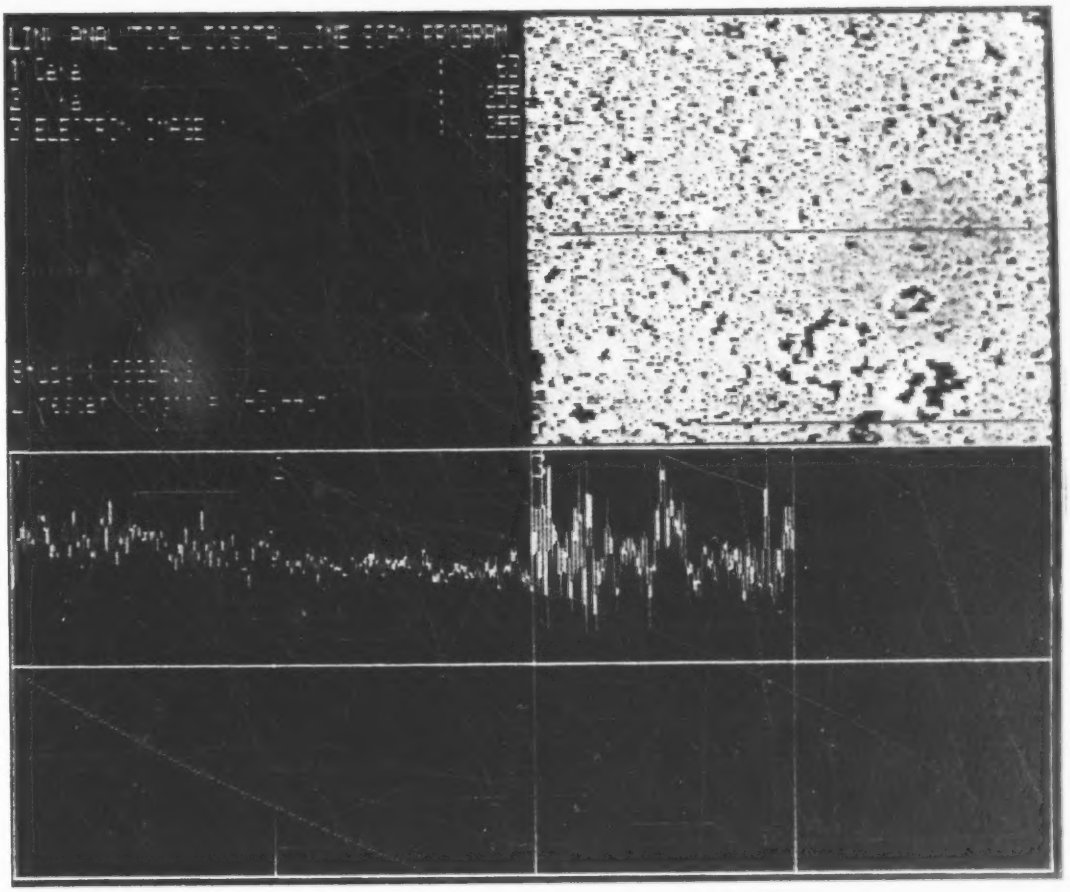

Figure 4.27 : EDX Traverses for Bitumen A

areas and the peripheral dark matrix.

It can be seen from these data that, V concentration remained fairly constant in all the three areas, but it was much higher compared to other catalysts as expected. The EDX traverses (Figure 4.27) supported these findings.

4.4.3 SEM Elemental Analysis by EDX for Silica A

Photomicrographs obtained from SEM did not show distinct rounded domains as was the case with Optical Microscope. However, there appeared to be three distinct regions based on their brightness levels. Some regions lacked a clear boundary, but showed the highest brightness, some regions had an intermediate grey level, and some regions were dark. An example section of each region was analyzed for its metals content and a general analysis was also performed. Table 4.8 gives these analyses.

To understand the disribution of metals in the distinct domains, the incident beam in EDX was moved along these distinct domains and peripheral dark matrix and changes in the metals concentrations were obtained as a result. Figures 4.28 shows the results of EDX traverses for Silica A. It can be seen from these data that, while the S and Ca concentrations increased from dark to bright region, the V concentration dropped. This fact was supported by EDX traverses (Figure 4.28) which clearly show peaks for S and Ca. However, results for V could not be confirmed with these traverses due to its very small concentration.

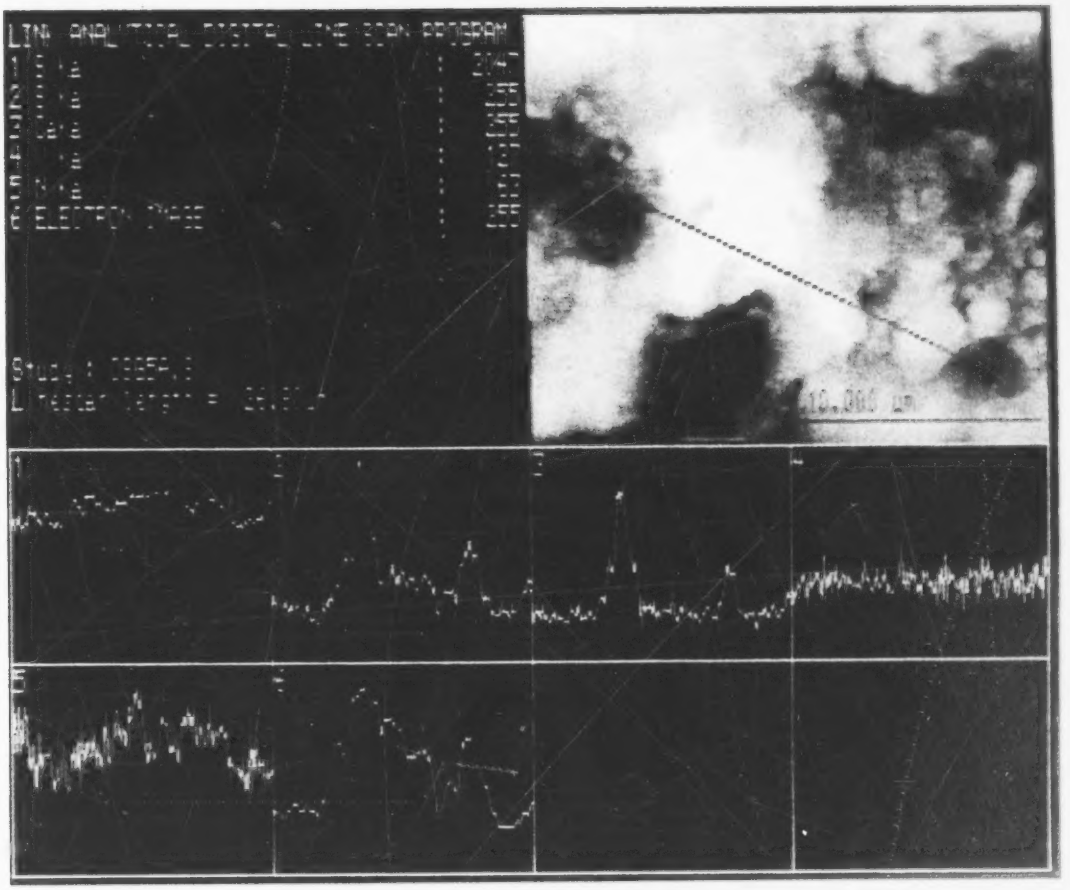

Figure 4.28 : EDX Traverses for Silica A

CHAPTER 5 : DISCUSSION

5.1. Heterogeneity in Carbonaceous Deposits

The optical microscopic examination revealed interesting information regarding the nature of the carbonaceous deposits. The reflectance microscopy of sectioned pellets showed that in some catalysts these deposits contained circular shaped, high reflectance domains indicative of higher aromaticity. The catalysts which showed these types of circular domains are listed in Table 4.1 and the relevant data about these catalysts is given in Section 3.1. The existence of these domains suggests that the coke deposition is non-uniform. This observation is significant because it establishes the fact that the coke deposition does not always follow a smooth gradient across the catalyst pellet but can occur in a fashion where coke preferentially gets deposited at some locations across the surface. Although this observation could be affected by the procedures employed in the preparation of samples, like grinding and polishing of the catalyst samples, the coke is intimately associated with the alumina matrix. The sample preparation procedures, therefore, would be unlikely to cause the formation of high-reflectance domains.

These bright domains were not observed in all the catalyst samples analyzed, however, they were found in a sufficient number of samples to establish a pattern in their formation. From Table 4.1 and Section 3.1 it can be seen that only those catalysts which were in use for a longer period of time (e.g. 18 to 24 months) developed these bright domains. Also, these bright domains were observed only the in case of catalysts which were being used to treat distillates containing some coked product in the feed. These two facts can be used to infer that bright spots would not likely to form in the catalysts used in shorter periods of service regardless of the feed they were being used to treat and also that coker distillates are somehow related to the formation of these bright spots.

It was also observed that there was a distribution of **dark** domains in case of

bitumen catalysts and that bitumen catalyst CSTR-2 exhibited fluorescence. These features were fainter after 15 hours and had completely disappeared in an 18 days sample. This observation could be due to the rapid adsorption of fluorophores (compounds that cause fluorescence) in a **heterogeneous** fashion and hence it indicates the existence of circular domains within the γ-alumina matrix.

These observations in the case of catalysts from coker distillates and bitumen suggest that heterogeneity in the distribution of coke may be a property of the alumina matrix, since alumina was a factor which was common in all the cases.

5.1.1 Anisotropy of Bright Domains

The bright domains exhibited anisotropy in only one catalyst, namely Naphtha A. However, it should be emphasized that only a few samples were analyzed for anisotropic characteristics, which were : Naphtha A, Naphtha B, MD-A, CSTR-2, CSTR-3, and Bitumen A. It was noted in Section 2.2.1 that liquid crystal formation is associated with anisotropic character, where the liquid crystal undergoes an ordered structural transformation and gives rise to anisotropic properties. Only one catalyst sample showed bright domains as well as anisotropy, therefore, anisotropic character was not a general characteristic of the coke domains and hence liquid crystal formation is not the only mechanism for the formation of these domains.

5.1.2 Fluorescence Characteristics of Bright Domains

Out of the series Naphtha A, Naphtha B, MD-A, CSTR-2, CSTR-3 and Bitumen A, only two catalyst samples showed fluorescence characteristics namely Naphtha A and CSTR-2. However, there was a difference in these characteristics. In the case of Naphtha A, the dark background matrix and not the bright domains showed fluorescence whereas in case of CSTR-2, the dark domains exhibited fluorescence. In both cases, the features were roughly circular with a diameter of *ca.* 20 μm. However, the Bitumen A and CSTR-3 catalysts did not show any fluorescent properties which suggests that the organics

adsorbed on the bitumen catalyst lost fluorescence properties over the period of time in service. Therefore, it can be perceived that fluorescence is observed with less aromatic coke deposits and as the aromaticity of the coke increases (as with service time), fluorescent properties are lost. This observation is consistent with the general chemical characteristics that cause fluorescence (Warner, 1986).

5.1.3 Size of Bright Domains

Table 4.4 lists the average areas of the bright domains observed in some of the catalysts. The bright areas ranged from 4.68×10^{-10} to 6.44×10^{-10} m^2. Given the relatively small number of domains observed in a particular sample (approximately 90-140), there was not a statistically significant difference in size of these domains among the different catalyst samples. Therefore, the average area of the bright domains in any catalyst sample was approximately 5.5×10^{-10} m^2 which corresponds to a mean diameter of *ca.* 20 μm. It can be seen from CSTR-2 photomicrograph of Figure 4.7 that the size of the dark domain observed in case of this catalyst was approximately of the same size.

5.1.4 Area Ratio of Bright Domains

Table 4.4 lists the area ratios of the bright domains observed in various catalyst samples. Due to the relatively small number of bright domains, it is difficult to estimate the error bounds, however, the area ratios fell into the following groups :

Naphtha A		MD-A		
or	≥	or	≥	Gas-oil A
Naphtha B		Gas-oil C		
(0.05-0.06)		(0.02)		(0.01)

5.1.5 Distance Distribution of Bright Domains

A distance distribution of these bright domains was observed in case of middle distillate (Catalyst MD-A) and gas-oil (Catalyst Gas-oil A) feeds. It was not observed in case of naphtha feed. The bright domains were predominantly concentrated near the periphery of the catalyst pellet. This observation suggests that the feed boiling over 177^0C (above the boiling point range of naphtha) tends to give coke domains which are affected by diffusion/reaction mechanisms. One explanation for this type of behavior may be that the precursors of coke forming reactions are not able to reach the centre of the pellet before reacting, and that diffusion of these precursors is the rate limiting step. This explanation assumes that the catalyst itself is homogeneous in terms of the effective diffusivity, which is a fairly reasonable assumption.

5.1.6 EDX Analysis Results in Case of Naphtha A

The bright domains were found to contain higher Ni concentrations compared to the dark matrix, however, this result could be an artefact since polishing of the surface may give rise to movement of the metal species. Therefore, there was not enough evidence to establish that there was higher concentration of Ni in bright domains. To ascertain this one could analyze fractured samples of the same catalyst sample.

5.2 Possible Causes of Heterogeneous Distribution of Coke

Depending on the observed results and the published literature, two types of mechanisms for coke formation are possible.

5.2.1 Mesophase Analogy

The various coking reactions give rise to large aromatic structures. These aromatic structures coalesce to form very large polycondensed aromatic sheets. These sheets can have limited solubility in the bulk oil and hence they can separate by phase separation and build in size as more and more sheets are separated by forming liquid crystal spherules in the porous structure. This mechanism predicts that the size of these spherules is dependent

upon the temperature and time-on-stream history of the catalyst sample. It also predicts that these spherules should give rise to anisotropic character since liquid crystal formation is associated with anisotropy.

5.2.2 Heterogeneity of Alumina Domains

It was noted in Section 2 that according to published literature there is a strength distribution of acidity in the alumina matrix and that the acidity of the alumina can be increased by treating it with fluoride or chloride ions. These acidic sites are known to promote active deposition of aromatic coke by catalyzing condensation and polymerization type of reactions via carbonium ion formation. The disribution of acid sites that is normally measured is on the atomic scale on the alumina surface. Within a catalyst pellet, a heterogeneous distribution of acidity with a length scale of 20 μm woud be expected to give heterogeneous coke domains. The observed domains of high reflectance would follow from this heterogeneous coking.

One possible source of heterogeneity is the powder used to prepare the catalyst pellets. If the powder particles had different levels of acidity, then the pellets prepared from the powder wpould exhibit heterogeneous domains. Data are lacking, however, on acidities of alumina at this length scale.

This mechanism hypothesizes that there is a formation of large polycyclic aromatic hydrocarbons (PAHs) starting from monoaromatics and these PAHs have limited solubility in the bulk phase owing to very large molecular weights. The interesting question that arises from this discussion is that given the right conditions whether these PAHs can also form liquid crystals and exhibit anisotropy.

5.2.3 Comparison between the Two Hypotheses

After a careful examination of the above two hypotheses, it is noted that the hypothesis involving the mesophase analogy faces serious problems in terms of the results obtained in the course of this study :

1. By the mesophase analogy hypothesis, the bright domains should exhibit anisotropic character irrespective of their service history. This prediction was found to be wrong and only one catalyst sample, namely Naphtha A showed anisotropic characteristics whereas Naphtha B and MD-A samples showed these bright domains but no anisotropy. This observation showed that anisotropy and hence liquid crystal formation was not a general characteristic of the coke deposits.

2. Since the liquid crystals grow by coalescence of aromatic structures, the size of these bright domains should continue to grow with time. This means that those catalysts which were in use for longer times should show larger bright domains than those which were in short service. The size of the domains would also be very sensitive to the feed characteristics. However, this was not the case. The bright domains from different catalysts having different service histories exhibited bright domains of approximately equal mean area i.e. the mean area of the bright domains was independent of the sample history.

3. The CSTR-2 catalyst sample showed dark domains of similar size and it was in service for two hours for upgrading bitumen. This observation suggests that some of the precursors of coke are adsorbed faster than others, without any observation of liquid crystals.

4. The catalyst samples were polished before their microscopic examination, which means that a cross-section of the porous network was examined by various optical microscopies. The existence of 26 μm bright domains inside the catalyst required that the liquid crystal spherules occupied a volume much greater than the largest pore. The anisotropic domains in the case of Naphtha A were of a length scale much larger than the pore size. This observation indicates that large scale ordering can occur in the catalyst matrix under special conditions.

In conclusion, based on the results, the hypothesis involving alumina domains appears to be more reasonable.

5.3 Development of Coke in Distillate Hydrotreating Catalysts

Based on the published literature and observations, a mechanism for development of coke in distillate hydroprocessing catalysts will be proposed.

Hydrotreating catalysts are often exposed to olefins and diolefins which are produced from cokers at higher temperatures of about 400^0-550^0C. Monoaromatics like benzene and dicyclobenzenes are also present in middle distillates. These olefins and monoaromatics can proceed through condensation-cyclization reactions as shown in Figure 5.1. Strong Lewis acidic sites present on the surface can accept an electron pair from olefins and in turn catalyze condensation reactions. These olefins are now positively charged and can undergo addition reactions with the monoaromatics present in the feed. These addition reactions would lead to cyclization or ring closure reactions. However, it would be necessary to have strong Lewis acidic sites present on the surface for this purpose since weak acidic sites would not be able to initialize these reactions. Once initiated, these ring closure reactions can take place in two ways :

a) a kinetically favoured, four carbon addition to the region with most π-bonds localization, called as, ortho ring closure, or

b) a thermodynamically favoured, two carbon atom addition to a bay region, called as peri ring closure.

The sequence, as shown in Figure 5.2, would proceed via the four carbon addition (ortho ring closure) first followed by two carbon addition (peri ring closure). This sequence can then be repeated. This sequence is called Naphthalene Zigzag Reaction Pathway and can proceed upto a point where a very large polycyclic aromatic structure would be formed. Sullivan *et al.* (1989) reported that the peri ring closure reaction was much more favoured than the ortho ring closure reaction in hydrotreating VGO. Hence only those polycyclic aromatic structures could exist which were formed by two carbon addition. Also, these polycyclic aromatics would be rich in H:C ratio compared to the feed

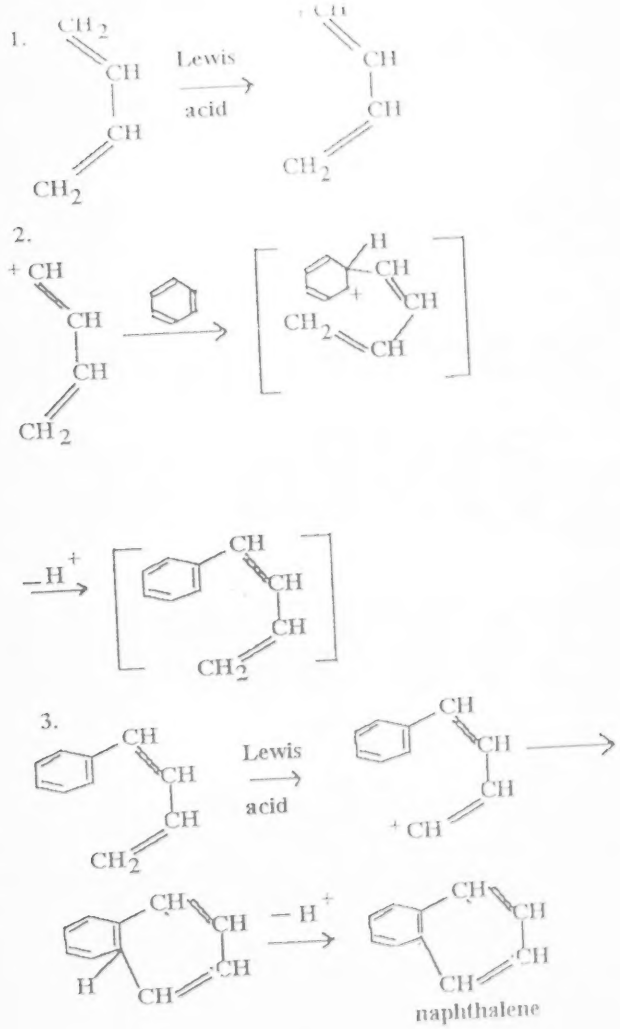

Figure 5.1 Condensation-polymerization Reactions between Monoaromatics and Olefins

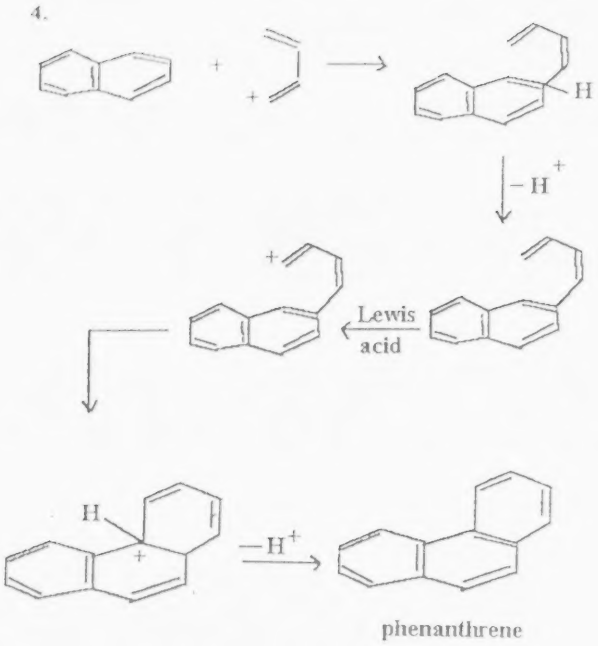

Figure 5.1 Continued....

Ortho-ring closure :

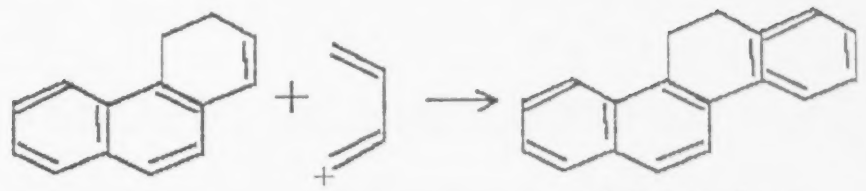

Triphenylene

Peri-ring closure :

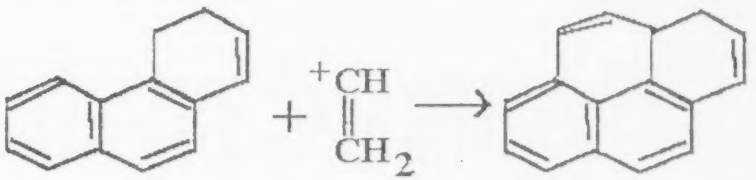

Pyrene

Peri-ring closure reactions are much more favored.

Figure 5.1 Continued .....

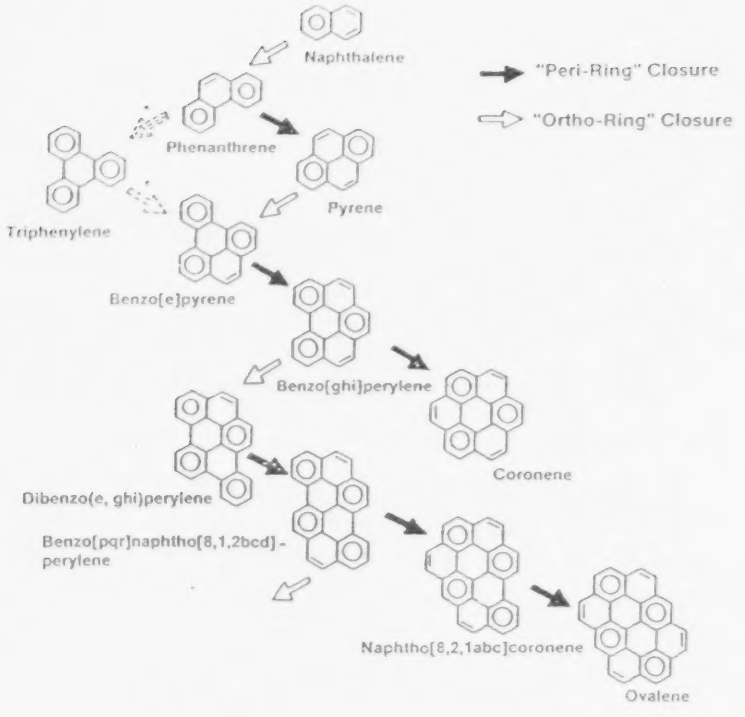

Naphthalene zigzag Reaction Pathway

Figure 5.2 Ring Closure Reaction Sequence

ratio. Thus starting from monoaromatics, very large polycyclic aromatics could be formed in hydrotreating of coker distillates.

5.3.1 Implications of Alumina Domains Mechanism in Case of Naphtha Catalysts

The observations in case of Naphtha catalysts can now be interpreted on the basis of acidic domains in alumina.

1. The higher the acidity of the alumina, the faster is the adsorption of coke precursors and rapid condensation-polymerization reactions. This would lead to a more aromatic coke i.e. bright domains in a shorter period of time. Also, as the service period of the catalyst increases, the less acidic domains also initiate the condensation reactions and there is a formation of coke all over the surface of the catalyst. This in turn can reduce the contrast between the dark matrix and the bright domains for example, see the reflectance measurements for Naphtha A and Naphtha B which show reduced contrast with higher total carbon content.

2. In case of naphtha catalysts, the olefins can initiate the above mentioned cyclization-polymerization reactions and these reactions can proceed to give large polycyclic aromatics. These aromatics would have a high molecular weight and hence a limited solubility in the aliphatic bulk phase. Thus there can be a phase separation from the bulk phase. Some confirmation of this type of phase separation has been provided by Sullivan *et al.* (1989) who reported presence of benzocoronenes (large aromatic structure) in the recycle streams from zeolite catalysts in hydroprocessing. These compounds were thought to be synthesized in reforming-type reactions. Large polycyclic aromatics can, therefore, exist in a liquid state and lead to a phase separation from the aliphatic oil, providing a starting material for mesophase growth and coalescence on the surface of the catalyst in case of naphtha catalysts. Since mesophase or liquid crystal formation is associated with anisotropy, one can expect naphtha catalysts to have the potential to exhibit anisotropic character.

Development of the anisotropic character requires a fluid state where, owing to the immiscibility in the bulk phase, the polycyclic aromatics would separate from the bulk phase and undergo structural transformation. However, another aspect of these reactions must be considered which is the cross-linking reactions. The heteroatoms present in the feed can develop non-polar free radicals which can cross-link the cyclization reaction products and enhance the free rotation tendencies of the products. This free rotation inhibits the formation of planar sheets of polycyclic aromatic molecules, and suppresses the formation and structural transformation of mesophase or liquid crystals on the surface of the catalyst.

Naphtha B catalyst had higher elemental C content than Naphtha A and Naphtha B also showed higher overall mean random reflectance values than Naphtha A although both were in service for the same period of time. Naphtha A was operated upstream at a higher H_2 partial pressure and also at somewhat lower temperature than Naphtha B. These operating conditions would have suppressed the dehydrogenation characteristics of the acidic domains, resulting in slower coke deposition and therefore the amount of coke deposited would be lower than Naphtha B. Our observations suggest that anisotropy is favored by slower coke deposition.

5.3.2 Implications of Alumina Domains Mechanism in Case of Gas-oil and Middle Distillates Catalysts

Gas-oils and middle distillates typically contain polycyclic aromatics which would be absent in naphtha feed. Therefore, there is a possibility of these aromatics undergoing cyclization-polymerization reactions, in the presence of acidic domains, similar to naphtha catalysts.

However, there is a possibility of greater cross-linking reactions in the case of gas-oils and middle distillates than in naphtha due to the higher heteroatom content. Apparently these cross-linking reactions and the higher degree of aliphatic substitution on

the aromatics did not favour the mesophase transformations and structuring, which would explain the absence of anisotropic character in the case of gas-oil and middle distillate catalysts.

The rate of formation of these cross-linked coke precursors can be an important factor in determining the existence of bright domains. Some of the commercial spent gas-oil (Gas-oil A and Gas-oil B) and all of the bitumen catalysts as well as laboratory gas-oil catalysts did not show any bright domains. If the rate of formation of cross-linked coke is too fast then coke deposition would occur throughout the catalyst pellet. No heterogeneity would be observable in this case, either in the form of bright domains or anisotropic characteristics.

The lack of heterogeneity in the laboratory gas-oil catalysts suggests two possible observations :

1. Although the literature suggests rapid coke deposition in the first few hours of operation, bright spots must develop over periods of time longer than 8 hours.

2. The commercial gas-oil (and possibly naphtha) catalysts which did not show bright domains, did not have a heterogeneous distribution of acidic domains.

The former hypothesis would be tested by examining gas-oil catalysts that were exposed to coker distillates for known periods of time, ranging from hours to months. The latter hypothesis could be tested by using fluorescent bases to examine the distribution of acid sites in fresh commercial catalysts, then correlating these results with the development of heterogeneous coke in reactor service.

From the distance distribution studies, it is obvious that in case of MD-A and Gas-oil A the bright domains were concentrated at the periphery of the catalyst pellet. This observation suggests that there was a diffusion/reaction mechanism at work and that the large polycyclic aromatics could not diffuse to the centre of the pellet before reacting. The high acidity domains may have adsorbed the aromatics before they reached the centre.

Another possibility is that the coke precursors could have been hydrogenated before reaching the interior of the pellets and hence could not form coke. The second hypothesis would be most likely to apply to olefins in the gas-oil and middle distillate.

5.4 Development of Coke in Residue Hydrotreating Catalysts

Residue hydrotreating catalysts are known to have substantially shorter life than naphtha and middle distillates hydrotreating catalysts, because of more extensive coke deposition along with deposition of metals. The mechanism presented for development of coke in section 5.3.1 is also applicable in residue hydroprocessing catalysts.

Bitumens are known to contain asphaltenes, resins and organometallic aromatics. The exact structure of asphaltene molecules is as yet unknown but asphaltenes are known to be present in a micellar form (Larson and Beuther, 1966) as shown in Figure 5.3. The straight lines represent the edge of flat sheets of continuous aromatic rings and the zig-zag configurations represent saturated chains of naphthenic rings. These sheets are separated by approximately 0.4 nm and are held together by a weak bonding (Larson and Beuther, 1966). Shibata *et al.* (1978) have shown that at the temperatures of processing of asphaltic feedstocks (350 - 450 ^{0}C) these micellar groups are largely disassociated into individual asphaltic molecules because the molecular motion at these temperatures overcomes the weak bonding that holds the micelle intact. It can now be proposed that these asphaltic molecules can get adsorbed on the acidic centres and get polymerized at these strong acidic sites present on the surface. Thus there could exist aggregates of dimers, trimers or tetramers on the surface in the form of planar sheets of aromatics. These individual asphaltic molecules themselves would be quite aromatic and this aggregation could lead to a limited solubility in aliphatic oils. This polymerization could result in the formation of a second liquid phase on the surface of catalysts. These aggregates should also have a very high ratio of C:H since they are essentially polyaromatics.

Since the acidic domains would adsorb basic polar species most strongly, and these

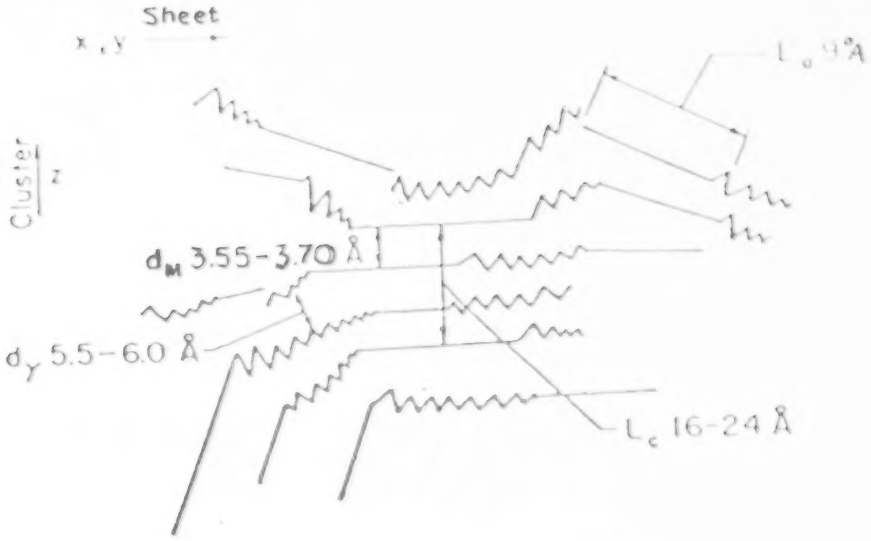

Cross-sectional View of an Asphaltene Model

represents the zig-zag configurations of a saturated carbon chain or loose net of naphthenic rings.

represents the edge of flat sheets of condensed aromatic rings

Figure 5.3 Asphaltenes in Micellar Form

polar compounds can be fluorophores, it can be expected that the coke deposits should exhibit fluorescence at short reaction times. This is confirmed by CSTR-2 catalyst which was used in bitumen upgrading for two hours and showed fluorescence. However, CSTR-3 catalyst which was used for the same feed but for 15.5 hours did not show any fluorescence. The reason can be that the coke levels in 15.5 hours reached higher levels of aromaticity and cross-linking than at 2 hours and this resulted in the loss of both fluorescence and any heterogeneity in the coke deposition. This observation indicates that fluorescence is observed only with less aromatic coke deposits and as the aromaticity increases fluorescence is lost.

5.5 Implications of Heterogeneous Coking

The observation that the coke deposits existed as highly aromatic domains in the catalyst porous structure can have major implications in understanding how coking reduces catalyst effectiveness. These deposits can reduce the active volume available for reactants and increase the length of diffusion path for the reactants since these domains must have a lower effective diffusivity.

If the domains are in fact due to heterogeneity of the γ-alumina powder, then careful attention must be paid to the preparation of the alumina.

Since these bright domains establish the fact that coke deposition is not uniform, average analyses of catalysts used to find the amount of coke and the aromaticity of coke using carbon content or ^{13}C-NMR may give misleading results.

Similarly, the residual carbon after regeneration is most likely to be found in the high-aromaticity domains.

CHAPTER 6 : CONCLUSIONS

The optical microscopic examination showed that five commercial spent catalyst samples (Naphtha A, Naphtha B, MD-A, Gas-oil A, Gas-oil C) and two laboratory spent catalyst samples (CSTR-2, CSTR-3) contained bright domains of high reflectance values, indicative of highly aromatic coke. The existence of bright domains suggested that the coke deposition was not uniform across the pellet, but was a localized phenomenon.

Only one catalyst sample (Naphtha A) showed anisotropy in the bright domains which suggested that the formation of mesophase or liquid crystal was not a general characteristic of the coke formation.

The size of the coke domains was approximately equal in all the catalyst samples, irrespective of the feed and reactor conditions, suggesting that coke deposition was intimately associated with the γ-alumina support matrix. Two catalyst samples had concentration of coke domains along the periphery of the pellet which suggested that reaction/diffusion mechanism played an important role in coke formation.

The development of heterogeneous coke deposition in middle distillate and residue hydrotreating catalysts was consistent with the presence of highly acidic sites of the γ-alumina matrix. According to the proposed mechanism for the development of coke, following conclusions could be drawn :

1. Since residual carbon after catalyst regeneration is most likely to remain in the heterogeneous domains, it should be advantageous to reduce the formation of these heterogeneous coke deposits.

2. The heterogeneity of the coke domains suggested that average analyses of catalysts used to find the amount of coke and the aromaticity of coke using carbon content or ^{13}C-NMR may give misleading results.

CHAPTER 7 : RECOMMENDATIONS FOR FUTURE WORK

7.1 Role of P and Ca in Modifying the Surface Properties

Addition of P has been shown to give higher HDN, cracking and isomerization activity with no effect on HDS activity (Weisser and Landa, 1973). However, there is a difference of opinion on how these additions change the active metal sites on the surface. Two possibilities have been proposed by Weisser and Landa (1973). One is that the addition of phosphate does not lead to an increase in the formation of the active "Ni-Mo-S" metal sulfide sites but rather leads to the formation of a new type of HDN site which is associated with phosphate. The other possibility is that addition of phosphate leads to formation of $AlPO_4$ or Ni-phosphate and thus changes the concentration of acid sites and acid strength. This view has been refuted by Papaioannou and Haynes (1990), who proposed that the addition of phosphate aids in the stacking of MoS_2 layers in Ni-Mo/Al_2O_3 catalysts by occupying part of the surface area and in the process exposes the Mo^{3+} sites believed needed for HDN.

It has been reported that Ca addition to Ni-Mo/γ-Al_2O_3 catalyst led to low acidity, stable activity, low coke-like substances formation and low N/C ratio in coke-like products (Masuyama *et al.*, 1990). The same researchers concluded that addition of alkali or alkaline earth ions neutralize the highly acidic sites and suppress the formation of coke-like substances.

Therefore, further study of the alumina matrix is desirable to determine if heterogeneous acidity can be detected in fresh catalyst, or whether it is the result of reaction conditions. One approach would be to label the acid sites using fluorescent bases and then examine the catalyst. Another approach would be to block the acid sites with Ca or an alkali metal and then study the changes in those acid sites and coke formation under different reaction conditions.

7.2 Regeneration of Spent Catalysts

Catalyst regeneration is needed once the activity of catalyst has decreased to such an extent that further operation is uneconomical. The efficiency of regeneration depends on conditions, especially temperature, encountered during the operation cycle, as demonstrated by Miertschin and Jackson (1970). Also, the coke forming tendencies of the feedstock have a marked effect on the regenerator performance (Rheaume and Ritter, 1976).

Another economically important factor in regeneration is the extent of coke removal. Because the removal of the last amount of coke is always the most expensive, reduction only to about 0.3 wt% coke is acceptable in many operations. However, the removal of the last amount of coke might be paid for by the gain of the catalyst activity (Rheaume and Ritter, 1976). For example, in a desulfurization study of a number of feedstocks, after the first *in situ* regeneration only 73% of the initial activity was recovered (Kassarjian, 1977). When the second in situ regeneration was followed by catalyst bed dumping, screening and reloading 90-95% of the initial activity was obtained. The third regeneration resulted again in a poor activity restoration.

These results suggest that it is very difficult to remove all the coke by regeneration. It is possible that coke deposited in the heterogeneous domains could be more difficult to remove than the coke deposited uniformly. Further study to understand the role of these heterogeneous domains in regeneration and ways to accelerate their removal is needed.

CHAPTER 8 : REFERENCES

Aguayo, A.T., Romero, A., Arandes, J.M., and Bilbao, J., "Effect of the Properties of Silica-Alumina Catalysts on Their Deactivation by the Deposition of Coke," *Intl. Chem. Engg.*, **27(4)**, October, 642 (1987).

Bakulin, R.A., Levinter, M.E., and Unger, F.G., "Coke Formation on Platinized Alumina Catalyst in Aromatization of Heavy Naphtha Cuts," *Int. Chem. Eng.*, **18**, (1), 89 (1978).

Bell, A.T., "Characterization of Carbonaceous Residues on Catalysts," *Catalyst Deactivation*, Eds. Petersen, E.E., and Bell, A.T., Marcel Dekker Inc., **30**, 235 (1987).

Beuther, A., Larson, O.A., and Perrotta, A.J., "The Mechanism of Coke Formation on Catalysts," *Catalyst Deactivation*, Eds.: Delmon, B., and Froment, G.F., **6**, 271 (1980).

Beuther, H., and Larson, O.A., "Role of Catalytic Metals in Hydrocracking," *Ind. Eng. Proc. Des. Dev.*, **4(2)**, 177 (1965).

Boorman, P.M., Kydd, R.A., Sarbak, Z., and Somogyvari, A., "Surface Acidity and Cumene Conversion 1. A Study of γ-Alumina Conyaining Fluoride, Cobalt, and Molybdenum Additives," *J. Catalysis*, **96**, 115 (1985).

Boorman, P.M., Kydd, R.A., Sarbak, Z., and Somogyvari, A., "Surface Acidity and Cumene Conversion. III. A Study of γ-alumina Containing Fluoride, Cobalt and Molybdenum Additives: The Effect of Sulfidation," *J. Catalysis*, **106**, 544 (1987).

Boorman, P.M., Kriz, J.F., Brown, J.R., and Ternan, M., "Proceedings, 4th Climax

International Conference : Chemistry and Uses of Molybdenum," Eds.: Barry, H.F., and Mitchell, P.C.H., 192 (1982).

Brooks, J.D., and Taylor, G.H., " Chemistry and Physics of Carbon," Ed.: Walker, P.L., Jr., Marcel-Dekker, New York, **4**, 243 (1968).

Brooks, J.D., and Taylor, G.H., "The Formation of Some Graphitizing Carbons," *J. Am. Chem. Soc.*, **3**, 185 (1965).

Butt, J.B., "Catalyst Deactivation," *Adv. Chem. Ser.*, **109**, 259 (1972).

Butt, J.B., "Catalyst Deactivation and Regeneration," *Catalysis:Science and Technology*, Eds. Anderson, J.R., and Boudart, M., **6**, **1** (1981).

Butt, J.B., Joyal, C.L.M., and Megiris, C.E., "The Poisoning of Catalysts : Experimental Observations and Modeling," *Catalyst Deactivation*, Eds. Petersen, E.E., and Bell, A.T., Marcel Dekker Inc., **30**, 3 (1987).

Choi, S.H.K., and Gray, M.R., "Structural Analysis of Extracts from Spent Hydroprocessing Catalysts," *Ind. Eng. Chem. Res.*, **27**, 1587 (1988).

Cimbalo, R.N., Foster, R.L., and Wachtel, S.J., "Deposited Metals Poison FCC Catalyst," *The Oil and Gas Journal*, **May 15**, 112 (1972).

Diez, F., Gates, B.C., Miller, J.T., Sajkowski, D.J., and Kukes, S.G., "Deactivation of Ni-Mo/γ-Al_2O_3 catalyst : Influence of Coke on the Hydroprocessing Activity," *Ind. Eng.*

Chem. Res., **29**, 1999 (1990).

Dubois, J., Agache, C., and White, J.L., "The Carbonaceous Mesophase Formed in the Pyrolysis of Graphitizable Organic Materials," *Metallography*, **3**, 337 (1970).

Egiebor, N.O., Gray, M.R., and Cyr, N., "^{13}C-NMR Characterization of Organic Residues on Spent Hydroprocessing, Hydrocracking, and demetallization Catalysts," *Appl. Catal.*, **55**, 81 (1989).

Fleisch, T.H., Meyers, B.L., Hall, J.B., and Ott, G.L., "Multitechnique Analysis of a Deactivated Resid Demetallation Catalyst," *J. Catal.*, **86**, 147 (1984).

Furimsky, E., "Catalytic Removal of Sulfur, Nitrogen and Oxygen from Heavy Gas Oil," *AIChE J.*, **25**, (2), 306 (1979).

Furimsky, E., "Catalytic Deoxygenation of Heavy Gas Oil," *Fuel*, **57**, 494 (1978).

Furimsky, E., "Deactivation and Regeneration of Refinery Catalysts," *Erdole & Kohle*, **32**, 383 (1979).

Gates, B.C., Katzer, J.R., and Schuit, G.C.A., "Chemistry of Catalytic Processes," Chemical Engg. Series, McGraw-Hill Book Co., 259 (1979).

Gray, R.J., and Cathcart, J.V., "Polarized Light Microscopy of Pyrolitic Carbon Deposits," *J. Nuclear Materials*, **19**, 81 (1966).

Kassarjian, R.R., Advances in Desulfurization of Petroleum Products, The Petroleum

Publ. Co., Tulsa, Okla., 21 (1977).

Kipling, J.J., Shooter, P.V., and Young, R.N., "Formation of Anisotropic Mesophase," *Carbon*, **4**, 33 (1966).

Knözinger, H., and Ratnasaamy, P., "Catalytic Aluminas : Surface Models and Characterization of Surface Sites," *Catal. Rev. Sci. Eng.*, **17**, 31 (1978).

Lipsch, J.M.J.G., and Schuit, G.C.A., "The CoO-MoO_3-Al_2O_3 Catalyst 1: Cobalt Molybdate and the Cobalt-Oxide Molybdenum Oxide System," *J. Catalysis*, **15**, 163 (1969).

Marsh, H., "Carbonization and Liquid Crystal (Mesophase) Development. Part 1: The Significance of the Mesophase During Carbonization of Coking Coals," *Fuel*, **52**, 205 (1973).

Masuyama, T., Kageyama, Y., and Kawai, S., "A Ca-modified Ni-Mo Catalyst for Hyprocessing of Coal Liquid Bottoms in Two-stage Coal Liquefaction," *Fuel*, **60**, February, 245 (1990).

Miertchin, G.N., and Jackson, R., "Optimum Utilization and Replacement Policies for Decaying Catalysts," *Can. J. Chem. Eng.*, **48 (6)**, 702 (1970).

Mills, G.A., Boedeker, E.A., and Oblad, A.G., "Chemical Characterization of Catalysts. 1. Poisoning of Cracking Catalysts by Nitrogen Compounds and Potassium Ion," *J. Am.*

Chem. Soc., **72**, 1554 (1950).

Mills, G.A., Boedeker, E.R., and Oblad, A.G., "Dynamic Structure of Oxide Cracking Catalyst," *J. Am. Chem. Soc.*, **72**, 1554 (1950).

Nance, D.M., "Catalytic Cracking Over Crystalline Aluminosilicates," *Ind. Eng. Chem. Prod. Res. Dev.*, **8 (24)**, 31 (1969).

Nashijima, A., Shimada, H., Yoshimura, Y., Sato, T., and Mastubayashi, N., "Deactivation of Mo Catalysts by Metal and Carbonaceous Deposits During the Hydrotreating of Coal-derived Liquids and Heavy Petroleums," *Catalyst Deactivation*, Eds. Delmon, B., and Froment, G.F., Elsevier Science Publishers B.V., **34**, 39 (1987).

Ozawa, Y., and Bischoff, K.B., "Coke Formation Kinetics on Silica-Alumina Catalyst," *Ind. Eng. Chem. Proc. Des. Dev.*, **7**, 67 (1968).

Papaioannou, A., and Haynes, H.W., "Alkali-metal and Alkali-earth Promoted Catalysts for Coal Liquefaction Applications," *Energy Fuels*, **4**, 38 (1990).

Pereira, C.J., "Metal Deposition in Hydrotreating Catalysts. 1. A Regular Perturbation Solution Approach," *Ind. Eng. Chem. Res.*, **29**, 512 (1990).

Pines, H., and Haag, W.O., "Radical Skeletal Rearrangement of Butylbenzenes over Chromia-Alumina Catalyst," *J. Am. Chem. Soc.*, **82**, 2471 (1960).

Rheaume, L., Ritter, R.E., Blazek, J.J., and Montgomery, J.A., "CO Combustion Catalysts - 1: New FCC Catalysts Cut Energy and Increase Activity," *Oil and Gas Journal*, May 24, 103 (1976).

Sanada, Y., Furuta, T., Kimura, H., and Honda, H., "Formation of Anisotropic Mesophase From Various Carbonaceous Materials in Early Stages of Carbonization," *Fuel*, **52**, April, 143 (1973).

Schlosser, E.G., "Catalyst Deactivation and Poisoning from a Chemical Engineering Viewpoint," *Intl. Chem. Engg.*, **17 (1)**, 41 (1988).

Sie, S.T., "Catalyst Deactivation by Poisoning and Pore Plugging in Petroleum processing," *Catalyst Deactivation*, Eds. : Delmon, B., and Froment, G.F., Elsevier Scientific Publ. Co., Amsterdam, 545 (1980).

Stach, E., Mackowsky, M.T., Teichmuller, M., Taylor, G.H., Chandra, and Teichmuller, D., *Coal Petrology*, Gebruder Borntraeger, Berlin, Stuttgart, 1982.

Stanulonis, J.J., Gates, B.C., and Olson, J.H., "Catalyst Aging in a Process for Liquefaction and Hydrodesulfurization of Coal," *AIChE J.*, **22 (3)**, 576 (1976).

Sullivan, R.F., Boduszynski, M.M., and Fetzer, J.C., "Molecular Transformations in Hydrotreating and Hydrocracking," *Energy and Fuels*, **3**, 603 (1989).

Tamm, P.W., Harnsberger, H.F. and Bridge, A.G., "Effects of Feed Metals on Catalyst Aging in Hydroprocessing Residuum," *Ind. Eng. Chem. Proc. Des. Dev.*, **20**, 262 (1981).

Ternan, M., Furimsky, E., and Parsons, B.I., "Coke Formation on Hydrodesulfurization Catalysts," *Fuel Proc. Technol.*, **2(1)**, 45, (1979).

Thakur, D.S., and Thomas, M.G., "Catalyst Deactivation in heavy Hydrocarbon and Synthetic crude processing : A Review," *Appl. Catal.*, **15**, 197 (1985).

van Doorn, J., Barbolina, H.A.A., and Moulijn, J.A., "Temperature Programmed Gasification of the Coke on Spent Hydroprocessing Catalysts with Oxygen and Hydrogen," *Ind. Eng. Chem. Res.*, **31**, 101 (1992).

Voorhies, A., Jr., "Carbon Formation in Catalytic Cracking," *Ind. Eng. Chem.*, **37**, 318 (1945).

Wanke, S.E., Szymura, J.A., and Ting-Ting Yu, "The Sintering of Supported Metal Catalysts : Experimental Observations and Modeling," *Catalyst Deactivation*, Eds. Petersen, E.E., and Bell, A.T., Marcel Dekker Inc., **30**, 65 (1987).

Warner, I.M., "Molecular Fluorescence and Phosphorescence," Eds. : Christian, G.D., and O'Reilly, J.E., Instrumental Analysis, Allyn and Bacon, 2nd Edition, 247 (1986).

Weinberg, V.A., and Yen, T.F., "Mesophase Formation in Coal-derived Liquid Asphaltene," *Fuel*, **61(4)**, 383 (1982).

Weisser, O., and Landa, S., "Sulfide Catalysts, Their Properties and Applications," Pergamon Press, Oxford, N.Y., 301 (1973).

White, C.E., and Argauer, R.J., *Fluorescence Analysis : A Practical Approach*, Marcel

Dekker Inc., New York, 1970.

Wukasch, J.E., and Rase, H.F., "Some Characteristics of Deposits on a Commercially Aged, Gas Oil Hydrotreating Catalyst," *Ind. Eng. Chem. Prod. Res. Dev.*, **21**, 558 (1982).

Yoon, W.L., Lee, I.C., and Kee, W.K., "Relationship Between Surface Acidity and Liquefaction Yield of Hydrotreating Catalysts," *Fuel*, **70**, January, 107 (1991).

APPENDIX I

The following tables give the frequency and area distribution data for each catalyst showing bright domains.

Table 1 : Frequency and Area Distribution Data for Naphtha A

Area range, $m^2 \times 10^{-11}$	Frequency	Number Fraction
0	2	0.01923
8	4	0.03846
16	15	0.1442
24	18	0.1731
32	6	0.05769
40	10	0.09615
48	5	0.04808
56	3	0.02885
64	12	0.1154
72	3	0.028846
80	6	0.05769
88	1	0.009615
96	3	0.02885
104	0	0.0
112	2	0.01923
120	1	0.00962
128	0	0.0
136	2	0.01923
144	7	0.06731
152	1	0.00962
160	0	0.0
168	4	0.03846
176	0	0.0

Table 2 : Frequency and Area Distribution Data for Naphtha B

Area range, m2 x 10-11	Frequency	Number Fraction
0	0	0.0
8	13	0.1008
16	17	0.1318
24	15	0.1163
32	12	0.09302
40	14	0.1085
48	8	0.06201
56	5	0.03876
64	9	0.06976
72	7	0.05426
80	5	0.03876
88	0	0.0
96	4	0.031
104	3	0.02326
112	0	0.0
120	3	0.02326
128	3	0.02326
136	2	0.0155
144	0	0.0
152	0	0.0
160	1	0.00775
168	9	0.06977
176	0	0.0

Table 3 : Frequency and Area Distribution Data for MD-A

Area range, m2 x 10-11	Frequency	Number Fraction
0	0	0.0
8	1	0.01695
16	0	0.0
24	1	0.01695
32	2	0.0339
40	3	0.05085
48	0	0.0
56	12	0.2034
64	17	0.2881
72	12	0.2034
80	6	0.1017
88	3	0.05085
96	1	0.01695
104	0	0.0
112	0	0.0
120	1	0.01695
128	1	0.0
136	0	0.0
144	0	0.0
152	0	0.0
160	0	0.0
168	0	0.0
176	0	0.0

Table 4 : Frequency and Area Distribution Data for Gas-oil A

Area range, $m^2 \times 10^{-11}$	Frequency	Number Fraction
0	0	0
8	0	0
16	0	0
24	1	0.04348
32	3	0.13043
40	1	0.04348
48	8	0.3478
56	4	0.1739
64	3	0.1304
72	2	0.08695
80	1	0.04348
88	0	0
96	0	0
104	0	0
112	0	0
120	0	0
128	0	0
136	0	0
144	0	0
152	0	0
160	0	0
168	0	0
176	0	0

Table 5 : Frequency and Area Distribution Data for Gas-oil C

Area range, $m^2 \times 10^{-11}$	Frequency	Number Fraction
0	2	0.03125
8	7	0.1094
16	12	0.1875
24	12	0.1875
32	10	0.1563
40	5	0.07813
48	4	0.0625
56	2	0.03125
64	1	0.01563
72	1	0.01563
80	1	0.01563
88	2	0.03125
96	1	0.01563
104	1	0.01563
112	3	0.04688
120	0.0	0.0
128	0.0	0.0
136	1	0.01563
144	0.0	0.0
152	0.0	0.0
160	0.0	0.0
168	0.0	0.0
176	0.0	0.0

Table 6 : Frequency and Distance Distribution for MD-A and Gas-oil A

Distance range, dimension less	Frequency MD-A	Frequency Gas-oil A	Number Fraction MD-A	Number Fraction Gas-oil A
0.5	0	1	0.0	0.07143
0.6	2	1	0.125	0.07143
0.7	2	2	0.125	0.1423
0.8	3	3	0.1875	0.2143
0.9	4	4	0.25	0.2857
1.0	3	1	0.1875	0.07143